ELSEVIER

Titanium- and zirconium-monosubstituted polyoxometalates as molecular models for studying mechanisms of oxidation catalysis

Oxana A. Kholdeeva [*], Raisa I. Maksimovskaya

Boreskov Institute of Catalysis, Pr. Ac. Lavrentieva 5, Novosibirsk 630090, Russia

Available online 18 August 2006

Abstract

Recent developments in the application of titanium- and zirconium-monosubstituted Keggin-type polyoxometalates (Ti- and Zr-POMs) as molecular models for studying mechanisms of H_2O_2-based selective oxidation catalysis are reviewed. The similarity in the catalytic behavior of Ti- and Zr-POMs and heterogeneous Ti(IV) and Zr(IV) single-site selective oxidation catalysts is demonstrated. The progress on the synthesis of Ti- and Zr-POMs, studying their interaction with H_2O and H_2O_2, and characterization of the peroxo species formed are surveyed, with special emphasis being placed on the role of protons in the activation of the peroxo species.
© 2006 Elsevier B.V. All rights reserved.

Keywords: Polyoxometalates; Titanium; Zirconium; Single-site catalysts; Hydrogen peroxide; Peroxo species; Oxidation; Mechanism

1. Introduction

The selective catalytic oxidation of organic compounds with low cost and environmentally friendly oxidants is of both fundamental and practical interest [1–27]. Nowadays, aqueous hydrogen peroxide is viewed as one of the most attractive oxidants from both ecological and economic standpoints, and this stimulates the search for efficient catalysts for H_2O_2 activation [2,5,8–15,20,22–29]. Numerous microporous and mesoporous materials, containing transition metal (TM) ions isolated in the framework of inorganic matrices or grafted (tethered) onto the surface, were prepared and examined in H_2O_2-based oxidations [2,5,7–12,14,15,29–45]. At the present time, it is widely recognized that titanium-containing molecular sieves are among the best catalysts for selective oxidations with hydroperoxides [2,8–12,14,15,28–39,43,45–47]. Microporous titanium-silicalite TS-1, discovered by the EniChem group at the end of 1970s, has opened a real perspective of H_2O_2 applications [7,12,14,15,29,48–53]. In the past decade, a considerable amount of research was dedicated to the development of mesoporous titanium-containing materials (Ti-HMS, Ti-MCM-41, Ti-MCM-48, Ti-MMM-2, etc.) capable of oxidizing large organic substrates [34–38,40,41,43–47]. Zr-containing molecular sieves, including microporous ZrS-1 [54] and mesoporous

Zr-HMS [55], Zr-MCM-41 [56,57], ZrO_2–SiO_2 [58,59], and Zr-MCF [60], have also demonstrated a pronounced catalytic activity in selective oxidation reactions with H_2O_2.

In the last years, more and more attention is given to molecular design of selective oxidation catalysts using a rational approach, which allows constructing on surfaces the active sites, uniform in composition and distribution [61–67]. However, for successful designing, fundamental knowledge about the nature of the active species is needed. The establishment of the so called "structure–reactivity relationships" is highly important to formulate requirements to composition and structure of an optimal catalytic centre. Despite the colossal achievements in surface science, investigation of mechanistic issues remains complicated in heterogeneous catalysis, for which the active catalytic species are normally difficult to investigate. Although considerable efforts, both theoretical and experimental, have been directed to rationalize activity observed in TS-1 and related materials [12,46,68–82], much remained to be understood regarding the nature of the active oxidizing species and chemical interactions at the molecular level. The same concerns other TM-containing molecular sieves. That is why mechanistic studies based on model soluble probes are becoming increasingly important in the catalyst designing area [83–91]. However, studying oxidation mechanisms using TM-complexes with organic ligands is complicated by their oxidative and hydrolytic degradation, polymerization and other processes [89,92]. TM-silsesquioxanes were suggested as homogeneous probes of heterogeneous single-site catalysts [83,86,88,93–98]. Titanium-silsesquioxanes have been

---

[*] Corresponding author. Fax: +7 3833 309573.
E-mail address: khold@catalysis.nsk.su (O.A. Kholdeeva).
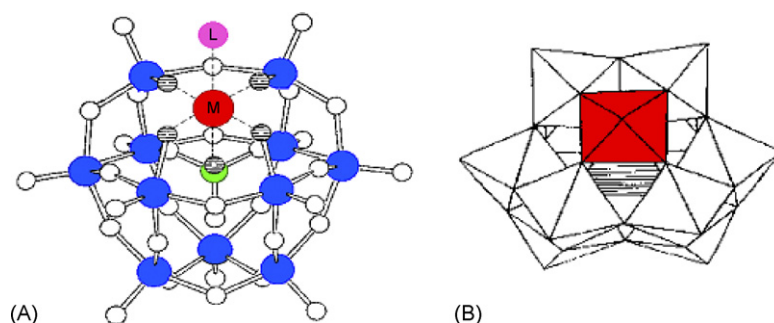
Fig. 1. Atomic (A) and polyhedral (B) representation of $[PM(L)W_{11}O_{39}]^{n-}$ (M-POM).

successfully employed for studying alkene epoxidation with alkylhydroperoxides [93–95,97,98]. Meanwhile, susceptibility to hydrolysis restricts the use of these compounds to anhydrous media, and this makes problematic their suitability for studying oxidations with H_2O_2.

In contrast to TM-complexes with organic and organometallic ligands, TM-substituted polyoxometalates (TM-POMs for short) are thermodynamically stable to oxidation and, furthermore, possess hydrolytic stability under appropriate pH conditions. Unique combination of properties has made this class of compounds very attractive for people working in different fields of chemistry, including catalysis and, in particular, molecular catalysis [20,25–27,99–109]. In 1986, Hill and Brown first revealed that some d-electron-TM-POMs (TM = Mn(II) and Co(II)) are remarkably effective catalysts for oxygen atom transfer from typical single oxygen donors, such as iodosylarenes and aniline N-oxide, to alkenes [110]. In the same year, Katsoulis and Pope demonstrated similar properties of Cr-POM [111]. These findings have allowed the authors to call TM-POM "oxidatively resistant inorganic analogues of metalloporphyrins" and found further development in subsequent numerous catalytic studies on TM-POM (many of them are cited in Refs. [25–27,100,101,103–109]). On the other hand, the apparent structural analogy of POMs and metal oxide surfaces allows one to view POMs as discrete, soluble fragments of extended metal oxide lattices [112–120]. A few research groups have used this approach for studying mechanisms of heterogeneous catalysis by TM-oxides and oxide-supported catalysts. Among the reported mechanistic studies were modeling of ammoxidation chemistry using the soluble MoO_3 analogue $[Mo_6O_{19}]^{2-}$ [121] and modeling methanol oxidation on MoO_3 using methoxo derivatives of polyoxomolybdates [122]. Finke and Droege reported that the trisubstituted heteropolytungstate dimer, $[Si_2W_{18}Nb_6O_{77}]^{8-}$, behaves as a solubilized piece of $(Nb_2O_5)_3$ [114]. Then Finke and co-authors demonstrated that $[HSiW_9V_3O_{40}]^{6-}$ can serve as a homogeneous model for H^+ mobility on a heterogeneous oxide surface [116]. Recently, Zr-containing polyoxotungstates have been suggested as soluble analogues of heterogeneous tungstated zirconia catalysts [123].

Given in mind the growing relevance of TM-single-site catalysts, TM-monosubstituted POMs are of special interest because they can function as soluble models of active TM catalytic centres isolated in an inorganic matrix. Indeed, the structural unit of the TM-monosubstituted Keggin-type heteropolytungstate

$[PM(L)W_{11}O_{39}]^{n-}$ ($PW_{11}ML$ for short), which is shown in Fig. 1, can be viewed as an ideal model of a single TM site. The $PW_{11}O_{39}^{7-}$ lacunary POM functions as a multidentate ligand for TM ion, which is strongly bound to four neighboring tungstens and one central P atom of POM through oxygen bridges. In fact, only external coordination position (positions, if coordination number of TM is higher than 6), which is occupied by ligand L, is labile and accessible for reactants. The presence of a phosphorous central atom offers additional advantage, namely the possibility of using ^{31}P NMR, which is a powerful techniques in POMs speciation and studying their dynamics in solutions.

In this short review paper we would like to summarize our experience in the synthesis, characterization and application of Ti- and Zr-POMs for studying mechanisms of H_2O_2-based oxidations [124–132]. The following subjects will be considered. First, we will compare catalytic properties of Ti- and Zr-POMs with catalytic properties of Ti,Si- and Zr,Si-materials in selective oxidation of a few representative organic substrates with H_2O_2. Then, we will discuss the progress on the synthesis and characterization of Ti- and Zr-monosubstituted Keggin-type heteropolytungstetes and studying their interaction with H_2O and H_2O_2. Finally, our recent accomplishments in the preparation and characterization of different type peroxo species formed upon interaction of Ti- and Zr-POMs with H_2O_2, determining their structure and the reactivity nature will be surveyed, with special attention being paid to the role of protons in the reactivity.

2. Catalytic properties of homogeneous M-POMs and heterogeneous M,Si-catalysts with M = Ti(IV) and Zr(IV)

To assess the applicability of Ti-POMs and afterward Zr-POMs for studying mechanisms of heterogeneous Ti- and Zr-single-site catalysis, we first compared the catalytic behavior of the POMs and the corresponding metal-silicates in oxidation of a few representative organic substrates, including two alkenes, cyclohexene (CyH) and α-pinene, 2,3,6-trimethylphenol (TMP), and two thioethers, methyl phenyl sulfide (MPS) and benzyl phenyl sulfide (BPS). Both the literature data and the results obtained in our group on heterogeneous Ti- and Zr-containing mesoporous silicates were used for the comparison.

The oxidation of CyH with H_2O_2 over Ti,Si-catalysts [55,133–141] and Ti-POMs [131,142–144] was studied by
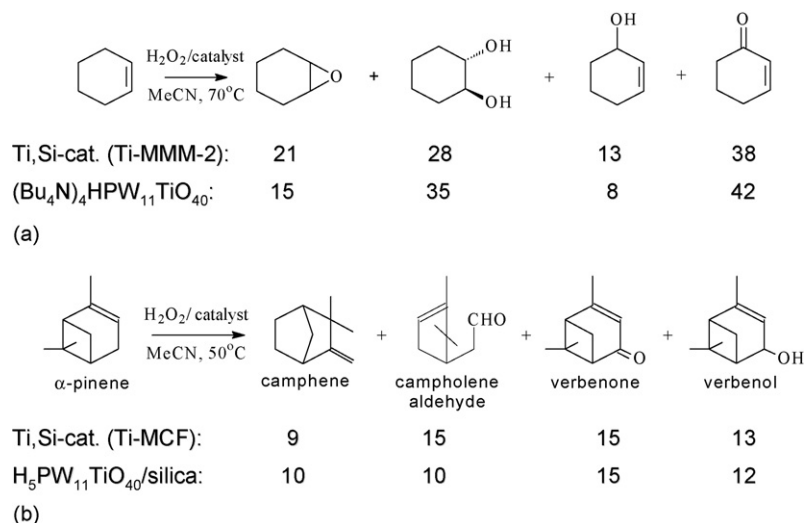
Fig. 2. Product distributions in oxidation of CyH (a) and α-pinene (b) over heterogeneous Ti,Si-catalysts and Ti-POMs [60,131].

several research groups. Normally, titanium–silicates produce products typical of both two-electron oxidation mechanisms (cyclohexene epoxide and *trans*-cyclohexane-1,2-diol) and one-electron oxidation mechanisms (2-cyclohexene-1-ol and 2-cyclohexene-1-one). The same set of CyH oxidation products was found with Zr,Si-catalysts [55,58]. The ratio between the products varied significantly depending on the hydrophobicity/hydrophilicity and other characteristics of the catalyst, solvent, reaction conditions, etc.

Initially, the results reported by different research groups on Ti-POM-catalyzed CyH oxidation looked quite contradicting. Some authors found rather good activity in CyH epoxidation [142,144], while others found none [143]. The reasons for that have become clearer in the light of several findings [127,131,145–147]. First, a few ^{31}P NMR studies have implicated that many POMs are solvolytically not stable to H_2O_2 and, in fact, they often act as precursors of the true catalyst, Venturello complex $\{PO_4[M(O)(O_2)_2]_4\}^{3-}$ (M=Mo, W), and/or other low nuclearity species [20,107,145–147]. The Venturello complex is well known as a very efficient epoxidizing agent [106,107,148,149]. Hence, before using any POM for studying mechanistic issues, ^{31}P NMR study must be carried out to confirm stability of the specific POM under real conditions of catalytic turnover. We performed such a study on Ti-POM and revealed that the solvent nature had a strong effect on solvolytic stability of POM to H_2O_2 and, therefore, on its catalytic behavior in alkene epoxidation. In fact, $PW_{11}Ti$ is stable with respect to at least 500-fold excess of H_2O_2 in MeCN: no products derived from degradation of the Keggin structural unit were detected by ^{31}P NMR in the range of +7 to −22 ppm. At the same time, it readily degrades in water and in two-phase systems, e.g. chlorinated solvent/water [127]. Furthermore, our recent study on CyH oxidation with H_2O_2/Ti-POM/MeCN system has revealed a high impact of the counter cations nature, specifically, of the number of protons in Ti-POM, on both the catalyst activity and selectivity [131].

We carried out CyH oxidation with H_2O_2 over the mesostructured titanium–silicate Ti-MMM-2 and monoprotonated *tetra-n*-butylammonium (TBA) salt of $[PW_{11}TiO_{40}]^{5-}$ [131] under comparable reaction conditions and found quite similar product distributions (Fig. 2a). Recently, we revealed that oxidation of α-pinene with H_2O_2 readily proceeds with both mesoporous Ti,Si-catalysts and Ti-POM (both homogeneous and immobilized in SiO_2 matrix) producing a similar set of oxidation products, consistent with a homolytic oxidation mechanism [60] (Fig. 2b).

The oxidation of CyH and α-pinene with H_2O_2 over Zr,Si-catalysts [55,58,60] and Zr-POMs [132] also has demonstrated similarity in the catalytic behavior of both types of the catalysts. Some results on α-pinene oxidation in the presence of both homogeneous and heterogeneous Ti- and Zr-single-site catalysts are presented in Table 1.

One can see that the yield of the allylic oxidation products, verbenol and verbenone, is quite similar for all the catalysts and depends mainly on the reaction conversion. The activity of both Ti- and Zr-POMs strongly depends on their protonation state. One can judge from the data of Table 1 that the activity of the highly protonated Ti- and Zr-POM catalysts expressed in TOFs is one order of magnitude higher than that of the corresponding M,Si-catalysts. In turn, the low-protonated Zr-POM demonstrates fairly low activity.

The oxidation of alkylphenols with H_2O_2 over mesoporous titanium–silicates [150–153] and Ti-POMs [129,130] has been intensively studied using TMP as model substrate. With both types of catalysts we found the same products, 2,3,5-trimethyl-1,4-benzoquinone (TMBQ, which is Vitamin E precursor) and 2,2′,3,3′,5,5′-hexamethyl-4,4′-biphenol (BP) (Scheme 1).

More recently, TMBQ and BP were found also with both Zr-POMs [132] and Zr-MSF [154]. Some typical results on TMP oxidation obtained under comparable reaction conditions in the presence of homogeneous and heterogeneous Ti- and Zr-catalysts are given in Table 2.

In general, the selectivity to TMBQ is higher for titanium single-site catalysts than for zirconium ones. With both homo-
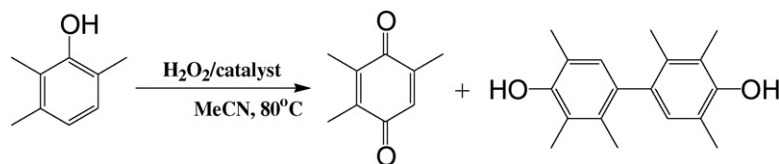
Scheme 1.

Table 1
α-Pinene oxidation with H_2O_2 in the presence of Ti- and Zr-catalysts[a]

Catalyst	α-Pinene conversion (%)	TOF_{av}[b] (h^{-1})	Verbenol yield[c] (%)	Verbenone yield[c] (%)
Ti-MCF[d]	46	1.5	22	17
Ti-POM[e]/silica	15[f]	23	37	45
Ti-POM[e]/silica	35	–	29	23
Zr-MCF[d]	55	1.4	15	15
Zr-POM[g]	40[f]	14	21	18
Zr-POM[h]	25[f]	8	n.d.[i]	n.d.
Zr-POM[j]	7[f]	0.8	n.d.	n.d.
Without catalyst	5[f]	–	n.d.	n.d.

[a] Reaction conditions: α-pinene, 0.1 mmol; H_2O_2, 0.12 mmol; MeCN, 1 mL; 30 °C; 5 h.

[b] TOF_{av} = (moles of substrate converted in the catalytic reaction − moles of substrate converted in the blank experiment)/(moles of M × h).

[c] GC yield based on α-pinene consumed. The main by-products are camphene, campholenic aldehyde and unidentified oligomeric/polymeric products formed due to overoxidation.

[d] Ti- and Zr-grafted on mesoporous cellular foams [60].

[e] Ti-POM = $H_5PW_{11}TiO_{40}$; catalyst contained 4.4×10^{-4} mmol Ti. The activity of the corresponding homogeneous system is quite similar [60].

[f] After 1 h.

[g] $(n\text{-Bu}_4N)_7H[\{PW_{11}O_{39}Zr(\mu\text{-OH})\}_2]$, 0.0025 M.

[h] $(n\text{-Bu}_4N)_8[\{PW_{11}O_{39}Zr(\mu\text{-OH})\}_2]$, 0.0025 M.

[i] Not determined.

[j] $(n\text{-Bu}_4N)_9[\{PW_{11}O_{39}Zr\}_2(\mu\text{-OH})(\mu\text{-O})]$, 0.0025 M.

Table 2
2,3,6-Trimethylphenol (TMP) oxidation with H_2O_2 in the presence of Ti- and Zr-catalysts[a]

Catalyst	TMP conversion (%)	TOF[b] (h^{-1})	TMBQ yield[c] (%)
Ti,Si-aerogel	100	78	85
Ti-MMM-2	100	66	81
Ti-MCF[d]	100	37	57
Ti-POM[e]	90	26	47
Zr-MCF[d]	83	31	49
Zr-POM[f]	90[g]	60	45
Zr-POM[h]	37[g]	32	n.d.

[a] Reaction conditions: TMP, 0.1 mmol; H_2O_2, 0.35 mmol; Ti, 0.006 mmol; MeCN, 1 mL; 80 °C; 5 h.

[b] Moles of TMP consumed/moles of M × h; determined from initial rates of TMP consumption.

[c] GC yield based on TMP consumed. The main by-product is BP.

[d] Ti- and Zr-grafted on mesoporous cellular foams.

[e] $(n\text{-Bu}_4N)_4HPW_{11}TiO_{40}$, 0.01 M.

[f] $(n\text{-Bu}_4N)_7H[\{PW_{11}O_{39}Zr(\mu\text{-OH})\}_2]$, 0.0025 M.

[g] After 1 h.

[h] $(n\text{-Bu}_4N)_9[\{PW_{11}O_{39}Zr\}_2(\mu\text{-OH})(\mu\text{-O})]$, 0.0025 M.

geneous and heterogeneous Ti-catalysts the product distribution strongly depends on the substrate to catalyst (Ti) molar ratio. The lower [TMP]/[Ti], the higher TMBQ yield [150,129].

Importantly, kinetic studies performed on the titanium–silica/H_2O_2 and Ti-POM/H_2O_2 systems have disclosed the same rate law [155,156]. First orders in both catalyst and oxidant and fractional (0–1) order in TMP were found for both types of catalysts. Such a kinetic behavior implies a mechanism that involves pre-association between phenolic substrate and titanium centre. The rate of both homogeneous and heterogeneous reactions decreases with decreasing H_2O concentration (is higher with 30% aqueous H_2O_2 than with concentrated H_2O_2) [150,155,156]. That is true not only for alkylphenol oxidation but also for alkene and thioether oxidations [126–128,131].

The oxidation of organic sulfide MPS with H_2O_2 smoothly proceeds at room temperature with both Ti,Si-catalysts [139,140,157,158] and Ti-POMs [124–128] to produce methyl phenyl sulfoxide (MPSO) and methyl phenyl sulfone (MPSO$_2$) with nearly quantitative yield (Scheme 2).

At the early stage of our research we found that some samples of Ti-POM showed high catalytic activity in the oxidation of MPS by H_2O_2, while other samples had very poor activity [124]. The strong effect of the composition of the cationic part of Ti-POM on its catalytic behavior has been revealed [124,125], and the crucial role of protons in the catalytic activity has been hypothesized [125,127]. The results on the product distribution attained with various Ti-containing catalysts, including protonated and non-protonated Ti-POM, are presented in Table 3.

Again, the product distribution is very similar for both Ti,Si-catalysts and Ti-POMs. Importantly, the MPSO/MPSO$_2$ ratio found for Ti-catalysts differs significantly from that typically

Table 3
MPS oxidation with H_2O_2 in the presence of Ti-catalysts[a]

Catalyst	MPS conversion (%)	TOF[b] (h^{-1})	MPSO yield[c] (%)	MPSO$_2$ yield[c] (%)
TS-2[d]	98	n.d.	78	22
Ti-MMM-2[e]	98	100	75	25
Ti-POM[f]	97	32	80	20
Ti-POM[g]	32	2.9	n.d.	n.d.

[a] Reaction conditions: MPS, 0.1 mmol; H_2O_2, 0.12 mmol; MeCN, 1 mL; 20 °C; 0.5 h.

[b] Moles of MPS consumed/moles of Ti × h.
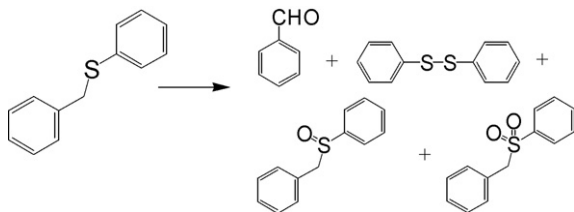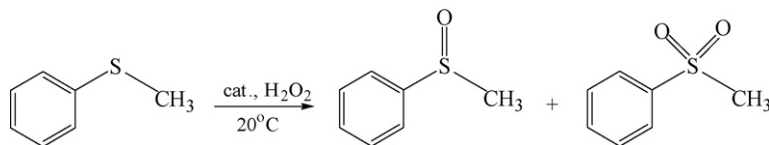
[c] GC yield based on TMP consumed.

[d] Reaction conditions see in Ref. [157].

[e] Mesostructured titanium–silicate catalyst [153].

[f] $[Bu_4N]_7[\{PTiW_{11}O_{39}\}_2OH]$, 0.0025 M.

[g] $[Bu_4N]_5[PW_{11}TiO_{40}]$, 0.005 M.

Scheme 2.

Scheme 3.

observed with V-catalysts, the latter being more selective with respect to sulfoxide formation [159–161].

The oxidation of benzyl phenyl sulfide (BPS), a test substrate frequently used to distinguish one- and two-electron oxidation mechanisms [162,163], with H_2O_2 in the presence of both mesoporous titanium–silicate Ti-MMM and Ti-POM affords benzaldehyde and disulfide along with the corresponding sulfoxide and sulfone (Scheme 3) [128]. Such a composition of products strongly supports a homolytic oxidation mechanism for both catalytic systems because benzaldehyde and disulfide most likely arise from a fragmentation of intermediate thioether radical cation [162].

Thus, based on the product and kinetic studies performed on several selective oxidations with H_2O_2 in the presence of M-POMs and mesoporous M,Si-catalysts (M = Ti, Zr), we have come to a conclusion that similar catalytic behavior of these two types of catalytic materials justifies the use of Ti- and Zr-POMs as soluble tractable probes for studying Ti- and Zr-catalyzed oxidation mechanisms.

3. Synthesis and characterization of Ti-POMs

Several well-characterized Ti(IV)-monosubstituted POMs have been known, including those having the Keggin [164–169], Dawson [170–172] and Lindqvist [173] structures. Among the Keggin Ti-POMs with P as a central atom, $[PTi(L)W_{11}O_{39}]^{n-}$,

those with $L = O^{2-}$ [164], Cp [165,166], Cl^-, OMe^- [167], and O_2^{2-} [168,169] had been reported when we started our activity in this field. Keggin Ti-POMs with Ga [174], Fe, Cr [175], and Co [176] central atoms were also documented. The initial confusion in the spectroscopic and catalytic results disclosed in the MPS and CyH oxidation with H_2O_2 over Ti-POMs has prompted us to a conclusion that along with the $PW_{11}Ti=O$ form described in the literature [164], some other forms may exist. In 2000, we fist reported the synthesis and characterization of the μ-hydroxo dimeric heteropolytungstate $[Bu_4N]_7[(PTiW_{11}O_{39})_2OH]$ and studied the monomer–dimer interconversion chemistry [127]. We suggested that acidification of a MeCN solution of $TBA_5PW_{11}O_{39}TiO$ first results in the protonation of the Ti=O bond to yield a Ti–OH species which dimerizes to produce a Ti–O–Ti dimer. The preferable protonation of Ti=O in titanium-monosubstituted POMs has been recently supported by computational studies [177]. Recently, we reported the synthesis of the μ-oxo-dimer $[Bu_4N]_8[(PTiW_{11}O_{39})_2O]$ as well as three monomer derivatives, $[Bu_4N]_4[PTi(L)W_{11}O_{39}]$, where $L = OH^-$, OMe^- and OAr^- (ArOH = TMP) [130]. Heteropolyacid $H_5PW_{11}TiO_{40}$ prepared by the electrodialysis method [130,178] was used as starting material for the syntheses (Scheme 4).

The Ti-POMs were characterized by the elemental analysis, IR, Raman, UV–vis, and multinuclear (^{31}P, ^1H, ^{183}W) NMR. It has been established that the dimeric and monomeric forms can be easily distinguished using IR (Fig. 3). The IR spectra of the dimers show a pronounced band at 640 and 655 cm^{-1} for the unprotonated and protonated POMs, respectively, which is characteristic of a Ti–O–Ti bond [127,130]. The dimeric structure was confirmed using FAB-MS technique [127].

The ^{31}P NMR study has revealed that several Ti-POMs show ^{31}P NMR signals having very close chemical shifts (Fig. 4). At the same time, the ^{183}W NMR spectra of all the Ti-POMs differ markedly in position of their six lines (Fig. 4). Thus,
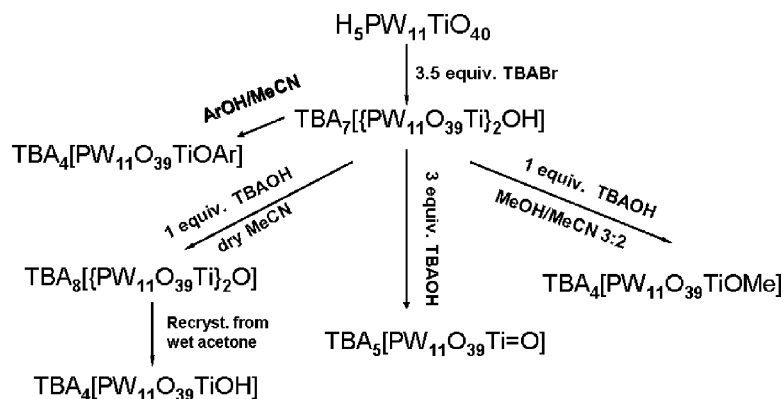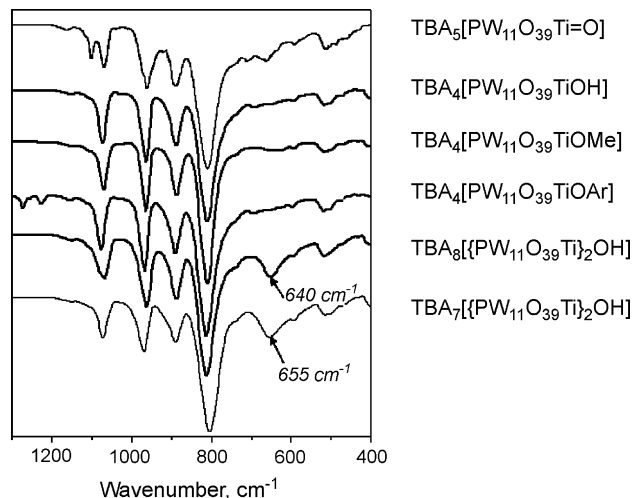

Scheme 4. Synthesis of Ti-POMs.

Fig. 3. IR spectra of Ti-POMs in KBr.

our work has demonstrated that reliable identification of various forms of Ti-monosubstituted Keggin-type POMs can be done only using a combination of the multinuclear NMR and IR data.

4. Ti-POMs with different Ti–L bonds and their interaction with H$_2$O$_2$

Although the ^{31}P NMR δ values of some Ti-POMs differ insignificantly, the δ difference and the signal sequence are reproducible and ^{31}P NMR allows one to distinguish between different Ti-POMs when some of them are present in equilibrium. Using ^{31}P NMR we studied interaction of Ti-POMs with H$_2$O and H$_2$O$_2$ in acetonitrile [130]. The rates of Ti-POMs hydrolysis were found to decline in the sequence (PW$_{11}$Ti)$_2$OH > (PW$_{11}$Ti)$_2$O $\gg$ PW$_{11}$TiOMe (TBA cations and oxygen atoms are omitted for short). In turn, the rates of the interaction of Ti-POMs with H$_2$O$_2$ followed the same order: PW$_{11}$TiOH $\gg$ (PW$_{11}$Ti)$_2$OH > (PW$_{11}$Ti)$_2$O $\gg$ PW$_{11}$TiOMe. The monomeric species with terminal Ti–OH bond showed the highest reactivity among the other Ti-POMs. Note that namely

tripodal Ti(OSi)$_3$OH species are believed to predominate on the surface of mesoporous titanium silicates [46].

Studies by ^{31}P NMR, IR, potentiometric titration, and cyclic voltammetry revealed that all the Ti-POMs, except for PW$_{11}$Ti=O, afford the same peroxo complex [Bu$_4$N]$_4$ [HPTi(O$_2$)W$_{11}$O$_{39}$] (**I**) upon interaction with aqueous H$_2$O$_2$ in MeCN. In sharp contrast to the other Ti-POMs, PW$_{11}$Ti=O reacts with H$_2$O$_2$ very slowly and yields the well-known inactive peroxo complex [PTi(O$_2$)W$_{11}$O$_{39}$]$^{5-}$ (**II**) [168,169]. This finding is in agreement with the proton-assisted oxo-peroxo exchange that has been established for titanyl *tetra*-4-pyridylporphyrin in the presence of H$_2$O$_2$ [179]. The comparative characterization of **I** and **II** will be given in the next chapter.

The catalytic activities of the Ti-POMs in TMP oxidation with aqueous H$_2$O$_2$ were found to correlate with the rates of the formation of **I** and the rates of the Ti-POM hydrolysis [130]. As we mentioned already, the oxidation rate decreased when concentrated H$_2$O$_2$ was used instead of dilute one [126,127,131,156]. This phenomenon was observed also with heterogeneous Ti,Si-catalysts [150,155]. The PW$_{11}$Ti=O species was practically inactive in both thioether [126,127] and alkylphenol [129] oxidation. All these findings collectively allowed us to suggest a two-step mechanism for the reaction of Ti-POMs with H$_2$O$_2$, which involves hydrolysis of the Ti–L bonds to yield Ti–OH species followed by its fast interaction with hydrogen peroxide producing titanium peroxo species **I** (Scheme 5).

The model study performed on Ti-POMs allowed to assess the reactivity of different Ti–L bonds, including Ti–OH, Ti=O, Ti–OMe, Ti–OAr, Ti–O(H)–Ti, and Ti–O–Ti, towards H$_2$O and H$_2$O$_2$, and to establish the relationship between this reactivity and catalytic activity of the Ti-POMs in TMP oxidation with aqueous H$_2$O$_2$. Using the values of equilibrium constants reported in [130] (some values are given in Scheme 5) one can roughly estimate the ratios between different Ti–L species in real reaction mixtures, containing Ti-catalyst, H$_2$O, H$_2$O$_2$, MeOH, and phenolic substrate.

Given all these in mind, a number of phenomena observed with both heterogeneous and homogeneous titanium catalysts can be understood and, therefore, predicted. For example, it
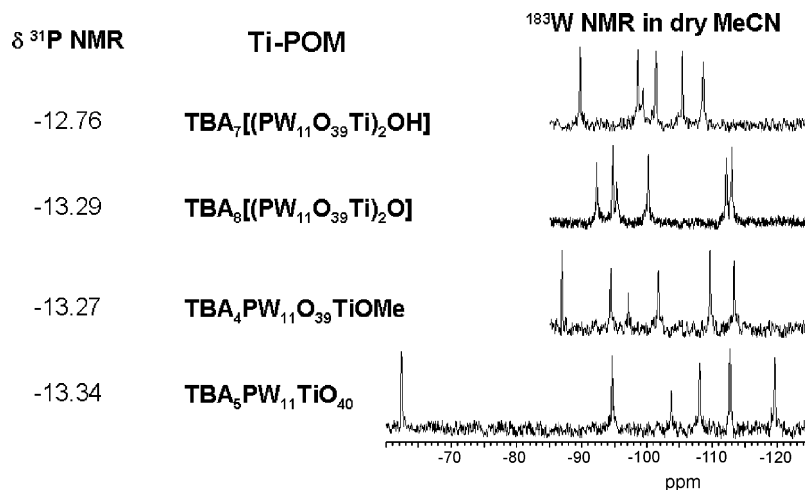
Fig. 4. ^{31}P and [183]W NMR data for Ti-POMs in dry MeCN.
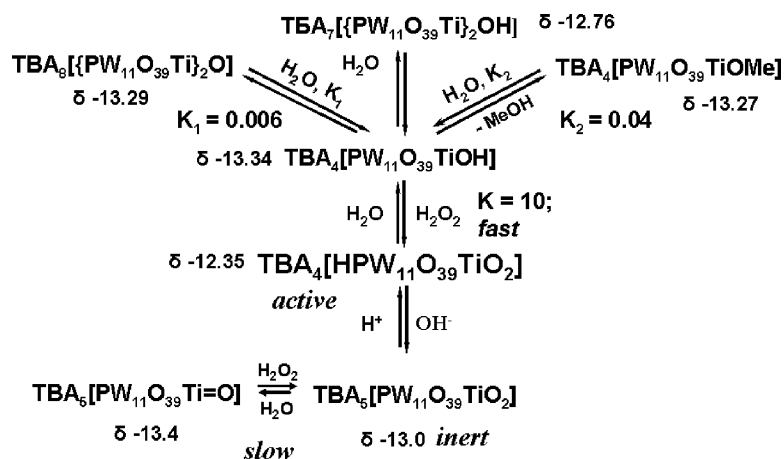
Scheme 5. Interaction of Ti-POMs with H_2O and H_2O_2.

becomes clear why catalysts containing titanyl (Ti=O) groups are not good for oxidations with H_2O_2; why basic additives deactivate Ti-single-site catalysts; why the oxidation rate decreases when concentrated H_2O_2 is employed instead of dilute one [126,127,131,150,155], etc.

It is worth noting that our conclusions based on model Ti-POMs are in good agreement with those based on the spectroscopic and theoretical studies on TS-1 and related materials. Thus, it has been inferred from the IR study using SO_2 as a chemical probe for titanyl groups that no Ti=O bonds are present in detectable concentrations in well-manufactured titanium–silicates [180]. X-ray absorption spectroscopy has also revealed no evidence for titanyl bond [61]. The key role of water as co-reactant in favoring the H_2O_2 adsorption at Ti sites and stabilizing titanium hydroperoxo complexes was deduced from spectroscopic and computational studies on the TS-1/H_2O_2/H_2O system [75,82].

5. Peroxotitanium complexes: the role of protons

5.1. Structure of monoprotonated peroxotitanium species I

Different structures of the active peroxotitanium species proposed for titanium–silicate catalysts are shown in Fig. 5. Both end-on (η_1) and side-on (η_2) binding modes of the peroxo ligand were suggested, but all the structures necessarily included an activating proton and thus corresponded to hydroperoxotitanium (protonated) rather than peroxotita-
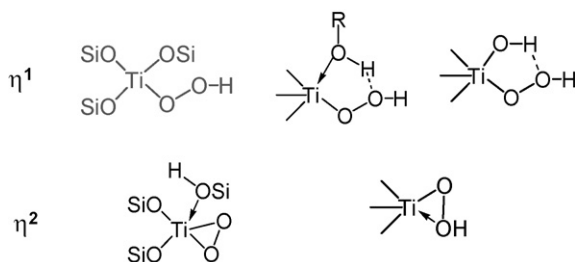
nium (non-protonated) complexes. At least two experimental observations were considered as arguments for that. First, it was found that basic additives deactivate both heterogeneous and homogeneous Ti-catalysts, while acid additives produce the opposite effect [12,46,51–53,181]. Second, all isolated and well characterized peroxotitanium complexes, including well-known peroxo complex **II** [168,169] and recently reported α-Dawson tri-peroxotitanium-substituted POM [α-1,2,3-$P_2W_{15}(TiO_2)_3O_{56}(OH)_3$]$^{9-}$ [182], appeared to be inactive toward oxidation of organic substrates (except for triphenylphosphine) in stoichiometric reactions [127,144,181–186]. At the same time, no hydroperoxotitanium complex was known.

Recently, we have succeeded in preparing the first protonated peroxotitanium complex, [Bu_4N]$_4$[$HPTi(O_2)W_{11}O_{39}$] or **I**, *via* interaction of the μ-oxo dimeric heteropolytungstate [Bu_4N]$_8$[($PTiW_{11}O_{39}$)$_2$O] with a 15-fold excess of 35% aqueous H_2O_2 in MeCN [129]. This compound has been isolated and characterized by elemental analysis, potentiometric titration, cyclic voltammetry, X-ray, IR, resonance Raman (RR), ^{31}P and ^{183}W NMR. Potentiometric titration with methanolic TBAOH confirmed the presence of one acid proton in the molecule of **I**. The addition of 1 equiv. of OH^- to **I** (^{31}P NMR: δ −12.4 ppm) resulted in the formation of **II** (δ −13.0 ppm). Iodometric titration indicated the presence of one peroxo group per molecule of **I**. Cyclic voltammetry study revealed that **I** has significantly higher redox potential ($E_{1/2} = 1.25$ V) compared to non-protonated **II** ($E_{1/2} = 0.88$ V). Therefore, protonation enhances the oxidizing ability of the peroxotitanium group. The ^{31}P and ^{183}W NMR spectra of **I** are presented in Fig. 6. The ^{183}W NMR spectrum of **I** consisted of six lines of 2:2:1:2:2:2 intensities pointing to C_s symmetry of the anion (or fast proton exchange on the ^{183}W NMR time scale). Both ^{31}P and ^{183}W NMR confirm the retention of the Keggin structural unit upon interaction of Ti-POM with H_2O_2.

The monomeric Keggin structure of **I** was confirmed also by single crystal X-ray analysis of **I** [129]. That is important because dimeric μ-peroxytitanium complexes have been precedented [187,188]. Unfortunately, the anion of **I** was statistically disordered due to the highly symmetric space group (I-4), and the position of the TiOO species was impossi-
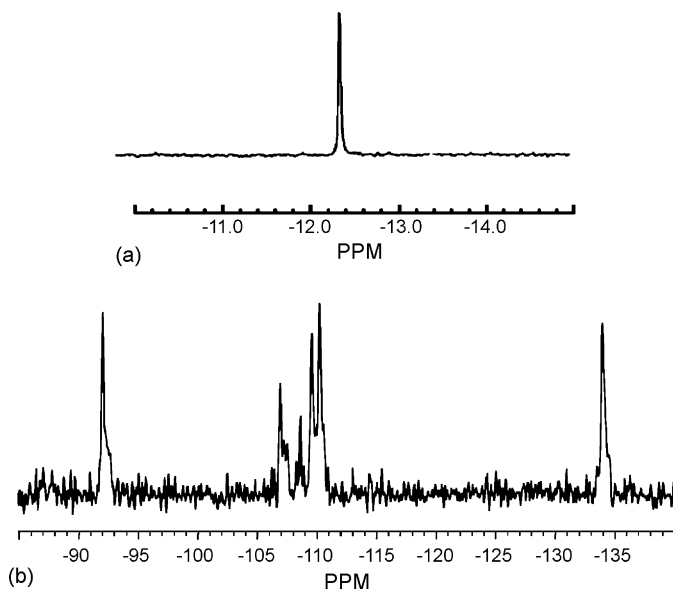

Fig. 5. The structures proposed for active peroxotitanium species in Ti,Si-catalysts [51–53].

Fig. 6. ^{31}P (a) and ^{183}W NMR (b) spectra of **I** in MeCN. (b) Reprinted with permission from Ref. [129]. Copyright 2004 American Chemical Society.

ble to determine. Earlier, Yamase's group faced the same problem when they performed an X-ray study on **II** ([(*i*-C$_3$H$_7$)$_2$NH$_2$]$_5$[PTi(O$_2$)W$_{11}$O$_{39}$]·4H$_2$O) [169]. Note that crystal disordering is a typical phenomenon for [XM'M$_{11}$O$_{39}$]$^{n-}$ heteropolyanions.

In contrast to the NMR spectra of **I** and **II**, which are extremely sensitive to protonation, both UV–vis and vibrational spectra of these peroxo complexes appeared to be quite similar [129]. The UV–vis spectra of **I** and **II** show a strong absorption with a maximum located at 395 and 390 nm, respectively, which is attributed to the O$_2$ → Ti ligand-to-metal charge transfer band [168,169]. Note that an absorption band having maximum at 361 nm was found upon dosing H$_2$O/H$_2$O$_2$ solution to TS-1 [68,75]. Characteristic features of the IR spectra of **I** and **II** (Fig. 7A) are two bands located at 630 and 690 and 620 and 714 cm^{-1}, respectively, which are absent in the IR spectra of peroxo-free Ti-POM (Fig. 3) and can be assigned to symmetric and asymmetric metal-peroxide stretches [129]. The O–O stretching band, which is anticipated to manifest around

900 cm^{-1} for monoperoxo complexes [171,189–191], is not seen in the IR spectra of **I** and **II** due to overlap with the strong W–O–W asymmetric stretch (895 cm^{-1}) of the Keggin unit.

The RR spectra of **I** and **II** taken with excitation at λ = 488 nm display an intense band at 630 cm^{-1}, which is lacking in the RR spectrum of the peroxo-free, colorless Ti-POM (Fig. 7B). This band shows strong resonance behavior, the intensity being gradually decreased with increasing excitation λ or upon slow decomposition of **I** [129]. Importantly, a strong band at 618 cm^{-1} has been revealed in the RR spectrum of TS-1 after treatment with H$_2$O$_2$/H$_2$O [76]. According to the literature, this band can be assigned to the symmetric Ti–O$_2$ stretching vibration of the peroxide group [192–195]. Therefore, the RR studies strongly support a side-on (η_2) structure of both **I** and the peroxotitanium species formed in TS-1. It is worth noting that an EXAFS study performed recently on the TS-1/H$_2$O$_2$ system also evidenced in favor of the side-on structure of the peroxotitanium species [68].

The question about the site of the activating proton in **I** has been addressed [129]. No IR bands were observed for solid **I** in the 1800–1600 cm^{-1} region indicating that no H$_3$O$^+$ was present and that the proton is directly attached to the POM surface [114,196]. The proton (OH) manifests in the IR spectrum of solid **I** at 3510 cm^{-1} [129]. Both the frequency and width ($\Delta\eta$ = 30 cm^{-1}) of the OH stretching band imply the presence of hydrogen bonding [197]. The possible protonation sites in **I** could be a peroxo oxygen atom and a Ti–O–W bridging oxygen [127]. The protonation of W=O and W–O–W oxygen atoms is less likely since metals with higher charge are more electron withdrawing, thereby decreasing the nucleophilicity of the oxygen atom at a given pH [198].

5.2. DFT calculations on **I** and **II**

The conclusions about the structure of **I** based on the experimental findings were in agreement with DFT calculations performed for **I** and **II** by J.-M. Poblet's group [129]. The electrostatic potential (EP) function [199,200] was used for discriminating the most of the least favorable protonation sites in **II**. The four oxygen atoms bridging the Ti and W atoms and the O–O group have been established as the most
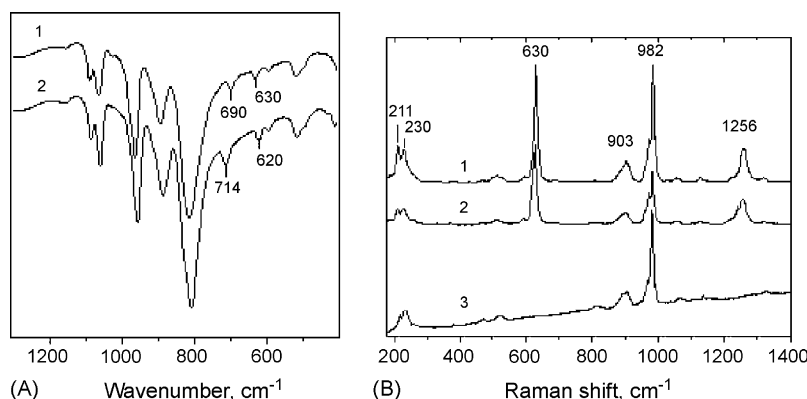

Fig. 7. FTIR (A, in KBr) and RR (B, λ$_{exc}$ = 488 nm) spectra of solid **I** (1) and **II** (2). (3) [TBA]$_5$[PTiW$_{11}$O$_{40}$]. Reprinted with permission from Ref. [129]. Copyright 2004 American Chemical Society.

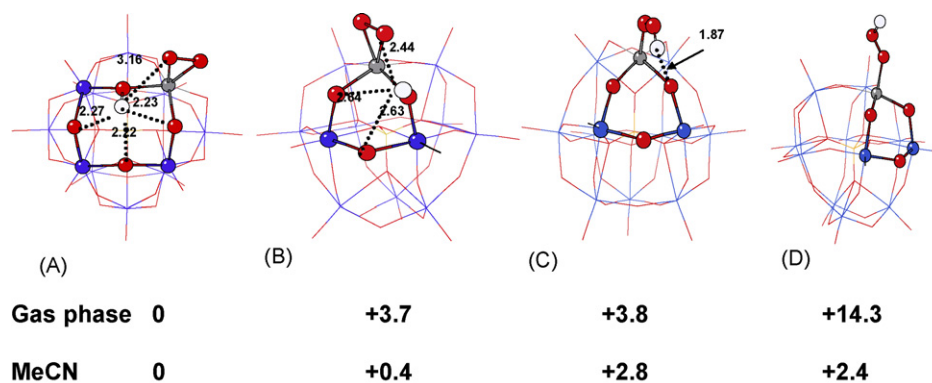|	(A)	(B)	(C)	(D)
Gas phase	0	+3.7	+3.8	+14.3
MeCN	0	+0.4	+2.8	+2.4

Fig. 8. Optimized structures, relative energies (in kcal mol^{-1}), and H···O distances (in Å) for several isomers of [HPTi(O$_2$)W$_{11}$O$_{39}$]$^{4-}$ [129]. Reprinted with permission from Ref. [129]. Copyright 2004 American Chemical Society.

likely positions to accept an incoming proton. The protonation of the terminal W=O bonds seems to be very unlikely [177,201]. The structure [PW(O$_2$)TiW$_{10}$O$_{39}$]$^{5-}$ was found to be 13.7 kcal mol^{-1} above the most stable (eclipsed) conformation for [PTi(O$_2$)W$_{11}$O$_{39}$]$^{5-}$. This excludes the W(O$_2$) peroxo complex as a result of the interaction of Ti-POM with H$_2$O$_2$.

The DFT study performed on the protonated species [HPTi(O$_2$)W$_{11}$O$_{39}$]$^{4-}$ revealed that in the most stable structure A (Fig. 8) the hydrogen is oriented towards the centre of the nearest M$_4$O$_4$ ring, a region with a high proton affinity [129]. In structure B, the proton is roughly equidistant from two bridging oxygens and from one of the oxygens of the peroxo group. This form is 3.7 kcal mol^{-1} above structure A in the gas phase. Protonation of the peroxo ligand was also thoroughly investigated. All attempts to obtain a TiOO–H side-on coordination structure were, however, unsuccessful because the optimization always evolved towards geometries with a η^1-coordination. This result contrasts with the recent B3LYP study on the Ti(OH)$_3$OOH model clusters which has found structures with a η^2-coordination for the OOH group [80]. This dissimilarity may be due to the different coordination number of titanium in the Ti-POM and Ti(OH)$_3$OOH as well as due to the different basicity of Ti–O–W and Ti–O–H bonds. The relative energy of η^1-structure C in relation to η^2-structure A is +3.8 kcal mol^{-1} in the gas phase. Structure D is quite unstable, presumably due to the lack of any stabilizing O–H interaction.

Importantly, the difference in the energies between all the structures considerably decreased when the solvent was included via a continuum model [202]. In MeCN (dielectric constant 37.0), the relative energies of structures B, C and D in relation to structure A are only +0.4, +2.8 and +2.4 kcal mol^{-1}. Therefore, although the calculations point to Ti–O–W as the most basic site, both Ti–OH–W and TiOO–H protonated species are expected to coexist in solution. The DFT calculations have clearly shown that, in addition to the intrinsic basicity of an oxygen site, inter and intra O···H interactions in POM clusters are of great importance in determining the protonation site.

The results of the DFT calculations prompted us to perform a RR labelling experiment using D$_2$O$_2$ instead of H$_2$O$_2$ for the preparation of I [129]. If the proton were attached to the peroxo group, a characteristic H/D downshift of the RR band would be

anticipated [203,204]. Nevertheless, the 630 cm^{-1} feature was not sensitive to the replacement of H for D. Therefore, the RR labelling experiment is in agreement with the DFT calculations and confirms that in solid I the activating proton is most likely localized at the Ti–O–W bridge rather than at the peroxo group.

5.3. Reactivity of I and II

As we have already mentioned, peroxo complex II is inactive toward oxidation of both alkenes [144] and thioethers [127] under stoichiometric conditions. At the early stage of our research, we generated I (δ −12.4 ppm) in situ by adding 1 equiv. of protons (in the form of triflic acid) to nonprotonated II (δ −13.0 ppm) in MeCN and studied its interaction with MPS using ^{31}P NMR and GC. Fig. 9 shows the generation of I and its gradual disappearance after addition of MPS. The disappearance of I directly parallels the formation of sulfoxide from the thioether, as detected by GC. To the best of our knowledge, this experiment was the first unequivocal demonstration of a direct stoichiometric reaction between a peroxotitanium complex and an organic substrate [126–128].

The kinetic study performed on the stoichiometric reaction between I and MPS has revealed that the reaction is first order in both reagents [126]. The linear dependence of the pseudo-first-order rate constant on the substrate concentration over a wide range of [S] implies that no strong binding between sulfide and I occurs. The stoichiometric oxidations of p-substituted phenyl methyl sulfides with I showed no Hammett free-energy correlation between the second-order rate constant and σ values. The interaction of I with BPS afforded a mixture of products shown in Scheme 3. Based on the product and kinetic studies, an outer-sphere electron transfer mechanism involving the formation of a thioether radical cation has been inferred.

Recently, we have found that I easily reacts with alkylphenols, specifically with TMP, to give products which are also consistent with a homolytic oxidation mechanism [129]. In particular, oxidation of TMP with I yields TMBQ and BP, the ratio between which depends on the TMP/I molar ratio (Scheme 6). When a two-fold excess of TMP was used, the main reaction product was BP (90%), while a two-fold excess of I produced presumably TMBQ (95%). This agrees with the reaction stoi-
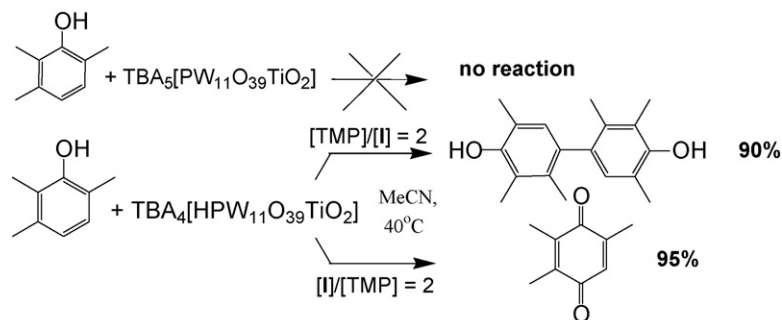
Scheme 6.

chiometry 2:1 and 1:2 for the TMP oxidation to BP and TMBQ, respectively. Again, unprotonated **II** was found to be inert.

The formation of BP, a typical one-electron oxidation product, implies a one-electron oxidation mechanism that implicates the formation of phenoxyl radicals ArO$^\bullet$. The radical coupling gives BP, while further interaction with **I** leads to TMBQ. As it has already been mentioned, the same products and analogous effect of the TMP/Ti ratio on the product distribution were found in the TMP oxidation with H_2O_2 catalyzed by mesoporous Ti,Si-catalysts [150–153].

The kinetic study of the stoichiometric reaction between TMP and **I** revealed fractional (0–1) order in TMP and thus supported

the formation of an intermediate which almost certainly had a η^1-structure and contained both peroxo moiety and phenol molecule (Scheme 7). The lack of kinetic isotope effect ($k_{ArOD}/k_{ArOH} = 1$) indicated that the rate limiting step of the reaction is most likely an inner-sphere electron transfer within this intermediate. The Ti-POM-based model study allowed us to suggest a general mechanism for alkylphenol oxidation with H_2O_2 over titanium single-site catalysts that implicates the reaction steps shown in Scheme 7.

The fate of phenoxyl radicals has been discussed above. The fundamental knowledge about the reaction mechanism helped us appreciably in optimizing the practically important process of TMBQ production over mesoporous Ti,Si-catalysts [205].

Keeping in mind the results on both the thioether and alkylphenol oxidation, we may conclude that **I** is a useful model compound for studying homolytic mechanisms of titanium-catalyzed oxidations. Again, the presence of proton in the molecule of **I** is crucial for its reactivity. One of possible explanations of this phenomenon is the increase of the redox potential of the peroxo group upon protonation (*vide supra*); however, we believe that proton may also facilitate the formation of the reactive η^1-intermediate shown in Scheme 7. Significantly, **I** is not reactive towards alkene epoxidation.

5.4. Diprotonatedperoxo titanium species III

Finally, we would like to address the question: what will happen if we increase the number of protons in the Ti-POM peroxo species? We had an observation that increasing proton

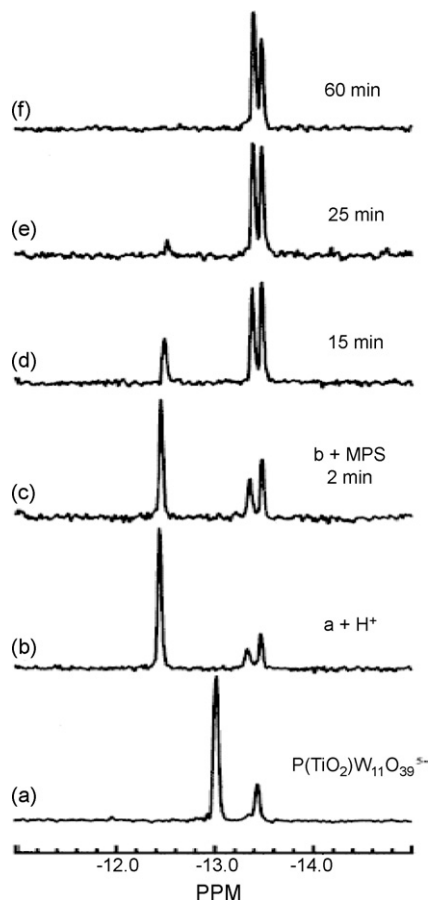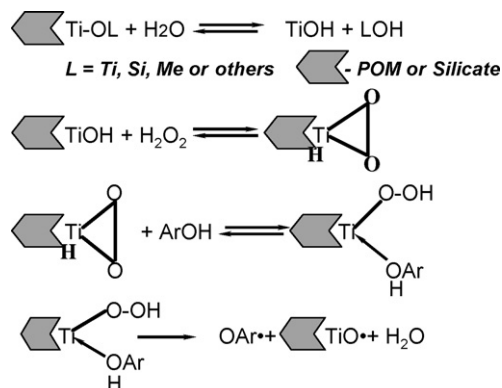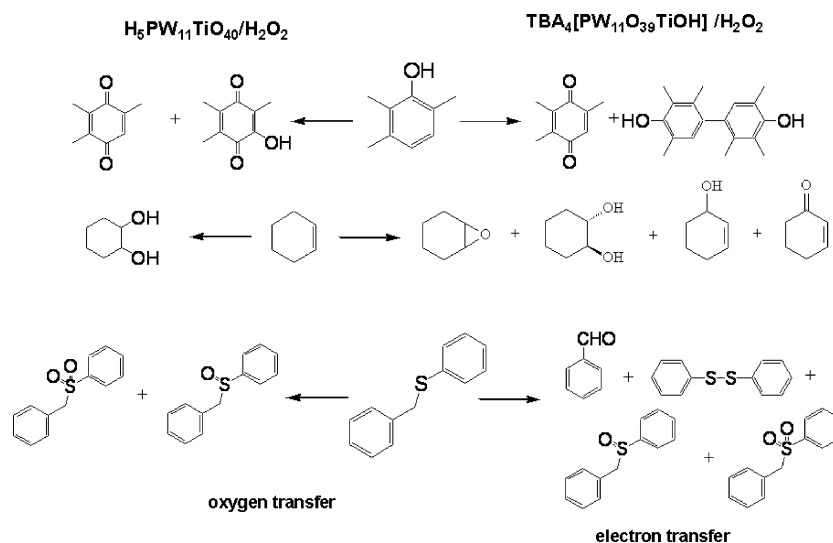Fig. 9. ^{31}P NMR spectra of $[Bu_4N]_5[PTi(O_2)W_{11}O_{39}]$ (**II**, 0.02 M) after addition of 1 equiv. of H$^+$ followed by addition of MPS (0.1 M). Reprinted with permission from Ref. [127]. Copyright 2000 American Chemical Society.

Scheme 7.

Scheme 8.

amount in Ti-POM results in appearance of products typical for heterolytic oxygen-transfer processes. Thus, when heteropolyacid $H_5PW_{11}TiO_{40}$ was employed as catalyst, no one-electron oxidation products were present (Scheme 8).

This phenomenon has been more carefully investigated using cyclohexene as substrate, and this study revealed that the increase in the number of protons in Ti-POM from 1 to 2 results in changing the reaction mechanism from a homolytic to a heterolytic one [131]. This manifests in increasing yield of the diol product at the expense of one-electron oxidation products, en-ol and en-one (Table 4).

In agreement with our results, Nomiya's group has confirmed recently very poor activity of dimer $[Bu_4N]_7[(PTiW_{11}O_{39})_2OH]$ in CyH epoxidation with H_2O_2 but found fairly good activity for $[Bu_4N]_7KH_2[(\alpha\text{-}1,2\text{-}PTi_2W_{10}O_{38})_2O_2]$ (two protons) and $[Bu_4N]_7KH_4[(\alpha\text{-}1,2,3\text{-}PTi_3W_9O_{37})_2O_3]$ (four protons) [206].

The ^{183}W NMR spectrum of $NaH_4PW_{11}TiO_{40}$ in the presence of an excess of H_2O_2 was consistent with C_s-symmetry and thus confirmed the retention of the Keggin structural unit

(Fig. 10). No low nuclearity species were detected by ^{31}P NMR in the range of +7 to −22 ppm upon addition of at least 100-fold excess of H_2O_2 to $H_5PW_{11}TiO_{40}$.

The stability of POMs towards solvolytic degradation in the presence of H_2O_2 is known to increase with increasing POM's charge [15,25]. So $[PW_{11}TiO_{40}]^{5-}$ is expected to be more stable than $[PW_{12}O_{40}]^{3-}$. The ^{31}P NMR study has implicated that a maximal protonation degree of $[PW_{11}TiO_{40}]^{5-}$ in MeCN is two [131]. Upon binding two protons, the charge of the Ti-POM becomes $3-$, and one might expect lowering resistance to H_2O_2. However, the certainly lower activity of $H_3PW_{12}O_{40}$, which is very prone to degradation by H_2O_2 [145–147], compared to $Na_{5-n}H_nPTiW_{11}O_{40}$ ($n = 2$–5) along with the ^{31}P and ^{183}W data indicate that the activity of Ti-POM is most likely not due to the low nuclearity species.

The change of the reaction mechanism upon increasing the number of protons in Ti-POM implies that most likely a diprotonated Ti-POM species, **III**, is responsible for the heterolytic oxygen transfer (Scheme 9).

Table 4
Cyclohexene (CyH) oxidation with 30% H_2O_2 catalyzed by POMs[a]

POM	CyH conversion (%)	Product yield[b] (%)			
		Epoxide	Diol	En-ol	En-one
$TBA_7[(PTiW_{11}O_{39})_2OH]$	26	4	9	2	11
$H_5PW_{11}TiO_{40}$	80	4	56	4	2
$H_5PW_{11}TiO_{40}$[c]	79	2	69	2	Trace
$NaH_4PW_{11}TiO_{40}$	84	6	63	2	4
$Na_2H_3PW_{11}TiO_{40}$	84	8	56	1	6
$Na_3H_2PW_{11}TiO_{40}$	75	8	54	2	5
$Na_4HPW_{11}TiO_{40}$	70	14	30	5	20
$TBA_3\{PO_4[WO(O_2)_2]_4\}$	96	81	10	Trace	4
–	4	2	Trace	1	0.3
$H_3PW_{12}O_{40}$[c]	41	25	14	1	Trace
$H_4SiW_{12}O_{40}$[c]	16	10	Trace	4	Trace

[a] Reaction conditions: CyH, 0.2 M; H_2O_2 (30%), 0.4 M; POM, 0.01 M; MeCN, 3 mL; 70 °C; 5 h.
[b] GC yield based on initial CyH.
[c] Ten percent H_2O_2 was used instead of 30% H_2O_2.

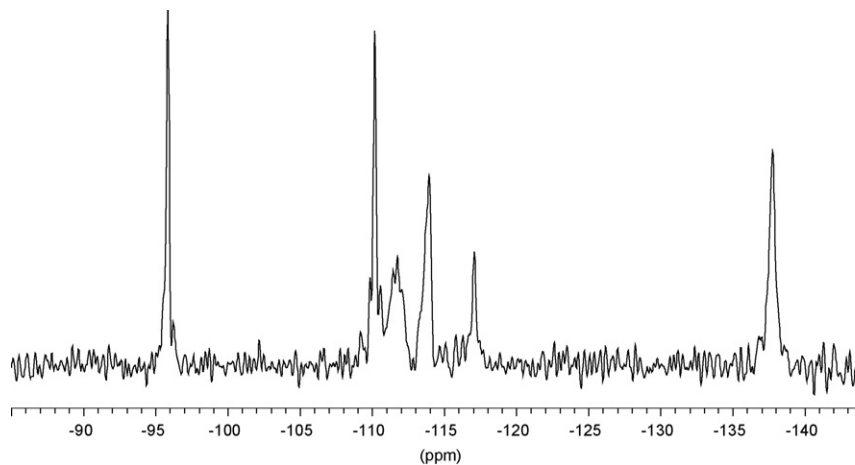Fig. 10. The ^{183}W NMR spectrum of **II** generated in situ *via* addition of a 15-fold molar excess of H_2O_2 to $NaH_4PW_{11}TiO_{40}$ (0.1 M in MeCN).

The stoichiometric reaction between CyH and **III** generated *in situ* by adding 1 equiv. of H^+ to a preliminarily cooled MeCN solution, containing **I** and CyH, was studied by both ^{31}P NMR (Fig. 11) and GC–MS. Upon addition of acid, the ^{31}P NMR signal of **III** ($\delta -12.14$) first arose (Fig. 11A), then its intensity rapidly decreased (simultaneously with the decoloration of the solution), and a signal at -12.56 ppm of the peroxo-free Ti-POM gradually appeared. The diol product was detected by GC–MS thus indicating that the decay of the signal of **III** is definitely due to the reaction between **III** and CyH.

Interestingly, when a small amount of water was added to a MeCN solution of **I** and CyH followed by addition of 1 equiv. of acid, a new peak at $\delta -12.65$ arose and disappeared simultaneously with the peak at $\delta -12.14$ (Fig. 11B) [131]. We assume that the signal with $\delta -12.65$ might belong to a hydrated form of **III**, which is also active towards oxidation of CyH. Possible structures of **III** are shown in Scheme 10.

The question about the localization of the second proton in the Ti-POM peroxo species is still open. The possible protonation sites are the peroxo oxygen atom attached to titanium and four Ti–O–W bridging oxygen atoms [129,201]. The RR and DFT studies performed on **I** and **II** implicated that at least one of the Ti–O–W bridges is protonated before the O–O group [129]. The second proton can be localized either at another Ti–O–W bridge (Scheme 10, structure **III**a) or at the peroxo oxygen (structures **III**b and **III**c). We believe that the drastic change in the reactivity of the Ti-POM peroxo complex toward CyH and the alteration of the reaction mechanism, both occurring after appearance of the second proton in the Ti-POM molecule, may indicate that
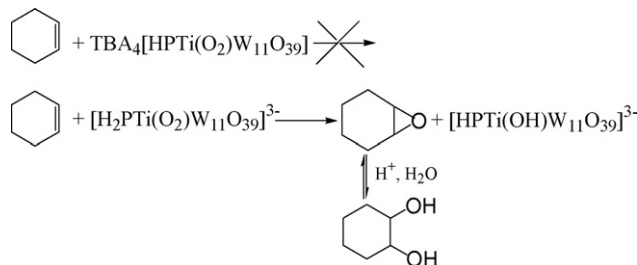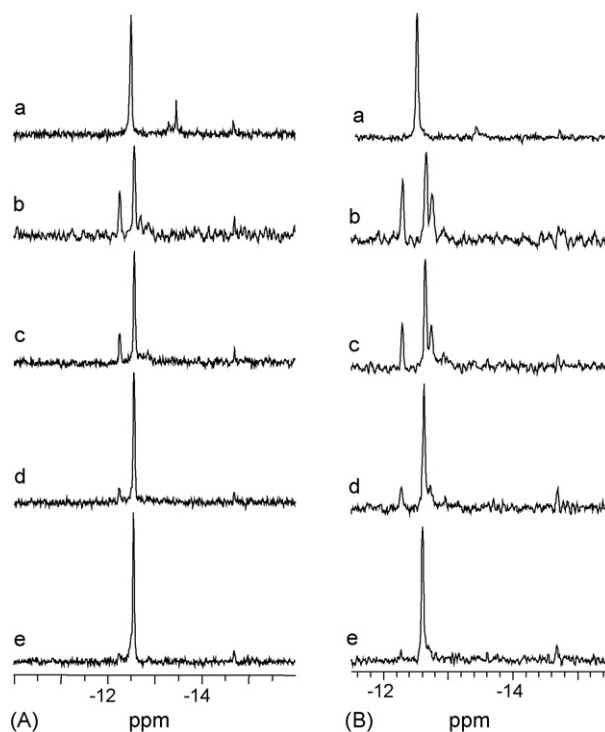
Fig. 11. (A) The ^{31}P NMR spectra of (a) $[Bu_4N]_4[HPTi(O_2)W_{11}O_{39}]$ (**I**, 0.02 M) + CyH 0.1 M; (b) immediately after addition of 1 equiv. of H^+ to (a); (c) after 1 min; (d) after 3 min; (e) after 8 min. (B) The same as (A), but with 28 μl (0.4 M) H_2O added to (a).
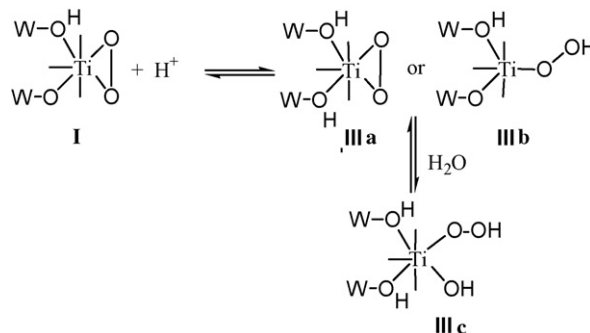
Scheme 9.

Scheme 10.

the second proton, in contrast to the first one, is bound to the peroxo oxygen thus activating the peroxo group to oxygen atom transfer. In solution, especially in the presence of some water, delocalization of protons (H_3O^+) between the Ti–O–W bridges and O–O group most likely occurs. Future experimental and theoretical studies would shed light on this matter.

As we mentioned already, the side-on structure of the active peroxotitanium complex was assumed based on both RR and EXAFS data [75,76]. Recently, the *in situ* XANES study on hydrated and anhydrous peroxo/hydroperoxo complexes on crystalline microporous and amorphous mesoporous titanosilicates has evidenced the equilibrium between side-on and end-on titanium peroxo complexes [81]. The amount of water is thought to be the key factor in the equilibrium displacement. Importantly, the results of our model study are in good agreement with the observation in heterogeneous Ti-single-site catalysis that tripodal titanium species Ti(OH)(OSi)$_3$ (one proton per one Ti atom) are more prone to operate via homolytic oxidation mechanisms, while tetrapodal Ti(OSi)$_4$ species have a propensity for heterolytic oxidation mechanisms [46]. The latter fact can be rationalized given in mind that hydrolysis of Ti–O–Si bond produces closely located Ti–OH and Si–OH groups and thus two protons can be supplied for the formation of the active peroxo species capable of oxygen transfer. In turn, introducing Al into mesoporous titanium silicates enhances Brőnsted acidity and thus favors the formation of two-electron oxidation products [207].

6. Synthesis and characterization of Zr-POMs

In the last years, Zr(IV)-containing POMs have attracted considerable attention, specifically as potential models for zirconia-supported tungsten catalysts [123]. Several well-characterized Zr-POMs, including Zr-monosubstituted monomeric [123,208] and dimeric [123,209] polyoxotungstates of the Lindqvist structure, composite polyoxotungstates, [Zr$_4$(μ_3-O)$_2$(μ_2-OH)$_2$(H$_2$O)$_4$(P$_2$W$_{16}$O$_{59}$)$_2$]$^{14-}$ containing polyoxo-zirconium clusters as bridging units [210] and enantiomerically pure {[α-P$_2$W$_{15}$O$_{55}$(H$_2$O)]Zr$_3$(μ_3-O)(H$_2$O)(L (and D)-tartH)[α-P$_2$W$_{16}$O$_{59}$]}$^{15-}$ [211] were reported. Following our interest to TM-single-site model catalysts we aimed at preparing and studying Zr-monosubstituted Keggin-type POM with P as central atom. Three new Zr-POMs differing in their protonation state, (n-Bu$_4$N)$_7$H[{PW$_{11}$O$_{39}$Zr(μ-OH)}$_2$] (**1**), (n-Bu$_4$N)$_8$[{PW$_{11}$O$_{39}$Zr(μ-OH)}$_2$] (**2**), and (n-Bu$_4$N)$_9$[{PW$_{11}$O$_{39}$Zr}$_2$(μ-OH)(μ-O)] (**3**) were synthesized starting from H$_5$PW$_{11}$ZrO$_{40}$ heteropolyacid (Scheme 11), which had been prepared by the electrodialysis method [178].

Compounds **1**–**3** were characterized by elemental analysis, potentiometric titration, X-ray single crystal structure, IR, Raman, ^{31}P and ^{183}W NMR spectroscopy [132]. The single crystal X-ray analysis of **2** has revealed that two Keggin structural units [PW$_{11}$O$_{39}$ZrOH]$^{4-}$ are linked through two hydroxo bridges Zr–O(H)–Zr with Zr(IV) in seven-fold coordination like it was previously found for the Lindqvist type dimer [123].

The IR spectra of **1** and **2** showed a characteristic band at 772 cm^{-1}, which moved to 767 cm^{-1} for **3** reflecting most likely
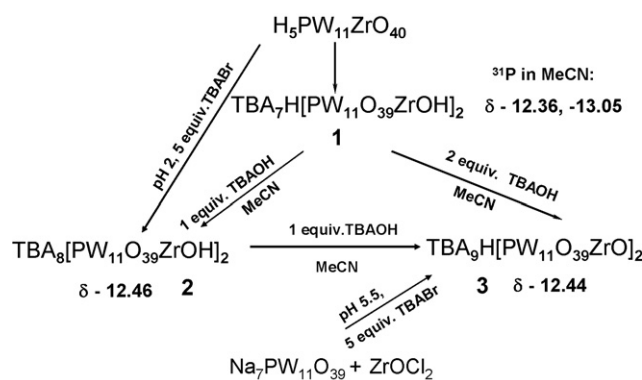
Scheme 11. Synthesis of Zr-POMs.

deprotonation of Zr–O–Zr bond. Potentiometric titration with methanolic Bu$_4$NOH indicates that **1**, **2** and **3** contain 2, 1 and 0 acid protons, respectively. The ^{31}P NMR spectra of **2** and **3** differ insignificantly in dry MeCN showing the only signal at δ −12.46 and −12.44 ppm, respectively. Their ^{183}W NMR spectra are also similar. Six lines with an intensity ratio approximately equal to 2:2:1:2:2:2 provide evidence for the C_s symmetry of **2** and **3**, which is in agreement with the X-ray single crystal analysis data. The ^{31}P NMR spectrum of **1** in dry MeCN contains two signals of comparable intensities: a narrow (∼3 Hz) peak at δ around −12.30 and a broad one (up to 50 Hz) at ∼−13.2 ppm (Fig. 12). The latter signal disappeared upon addition of activated 3A molecular sieves or small amounts (0.25–1.0 equiv.) of TBAOH. Both signals arise from dimer **1**, and their appearance is caused by the localization of the third proton in one of its sub-units, which makes them non-equivalent, and by the slow, on the NMR time scale, proton exchange in the absence of water. A similar phenomenon was observed by Finke et al. [116] for the ^{29}Si signal of TBA$_4$H$_3$SiW$_9$V$_3$O$_{40}$ in dry MeCN. In the presence of added H$_2$O the mobility of the protons increases and the mutual site exchange process accelerates, which results in the narrowing of the signal of the protonated sub-unit and its averaging with the signal of the other half (Fig. 12).

The conclusions based on the ^{31}P NMR data were completely confirmed by the ^{183}W NMR spectra of **1** in MeCN with variable H$_2$O content (Fig. 13). In dry solvent, instead of six signals, observed for **2** and **3**, dimer **1** gives nine broadened signals with the approximate intensity ratio 4:2:4:2:(4+2):2:1:1. Upon addition of H$_2$O, three latter more broadened and shifted upfield signals coalesce into one broad peak which tends to the W(4) resonance in the spectra of **2** and **3**, while the two other signals of the intensity 2 also coalesce into one signal corresponding to atoms W(1). W(1) and W(4) are linked with Zr by bent (1) and quasi-linear (4) W–O–Zr bridges. The observed splitting, shift and broadening of the signals indicate that the proton is localized on one of the four W(4)–O–Zr bridges of dimer **1**. The resulting distortion of the structure causes splitting of the peaks, more pronounced for the nearest W atoms. For the more distant W atoms the splitting manifests as the noticeable signal broadening. In the presence of added H$_2$O the site exchange rate increases which results in tending the complicated ^{183}W NMR spectrum to a typical six-line pattern (Fig. 13).
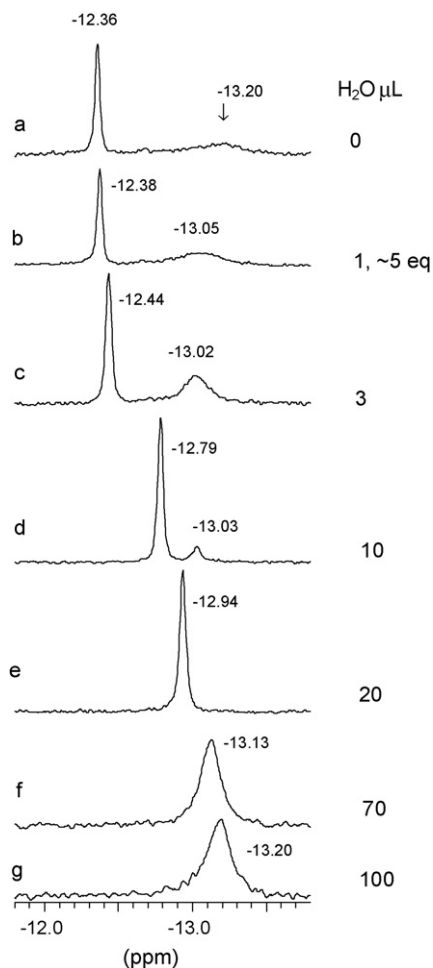
Fig. 12. The ^{31}P NMR spectra of $(n\text{-Bu}_4\text{N})_7\text{H}[\{\text{PW}_{11}\text{O}_{39}\text{Zr}(\mu\text{-OH})\}_2]$ (0.05 M) as a function of added H_2O to an initially dried MeCN solution at 20 °C.

Fig. 13. The ^{183}W NMR spectra of Zr-POMs (0.05 M, 20 °C): **3** (a), **2** (b), **1** in MeCN/H$_2$O (c), and **1** (d). Spectra a, b and d were run in dry MeCN.

7. Interaction of Zr-POMs with H$_2$O and H$_2$O$_2$ and catalysis of H$_2$O$_2$-based oxidations

The interaction of **1–3** with H_2O and H_2O_2 in MeCN has been studied by both ^{31}P and ^{183}W NMR [132]. The stability of the $[\text{PW}_{11}\text{O}_{39}\text{ZrOH}]^{4-}$ structural unit toward at least 100-fold excess of H_2O_2 in MeCN was confirmed by both NMR and Raman spectroscopy. The ^{31}P NMR study revealed that the interaction of **1** and **2** with H_2O in MeCN produces most likely monomeric species $(n\text{-Bu}_4\text{N})_{3+n}[\text{PW}_{11}\text{O}_{39}\text{Zr}(\text{OH})_n(\text{H}_2\text{O})_{3-n}]$ ($n = 0$–1) showing a broad ^{31}P NMR signal at -13.2 ppm (Fig. 12), while the interaction of **1** and **2** with H_2O_2 in MeCN leads to the formation of an unstable peroxo species showing ^{31}P resonance at δ -12.3 ppm and the six-line ^{183}W NMR spectrum (Fig. 14). The signal broadening may be due to the exchange between complexes containing different amount of water and peroxo groups. Our preliminary attempts to isolate the peroxozirconium species and to establish its structure failed due to fast dismutation of H_2O_2 in the presence of Zr-POMs. Note that significant H_2O_2 decomposition is also typical of heterogeneous Zr,Si-catalysts [59]. Using ^{31}P NMR and GC–MS we have demonstrated that this species reacts rapidly with cyclohexene producing 2-cyclohexene-1-one and *trans*-cyclohexane-1,2-diol.

Both **1** and **2** show a pronounced catalytic activity in H_2O_2 decomposition and H_2O_2-based oxidation of organic substrates, including cyclohexene, α-pinene and 2,3,6-trimethylphenol (see Tables 1 and 2). The oxidation products are similar to those observed over heterogeneous Zr,Si-catalysts [54–60] and, even for $\text{H}_5\text{PW}_{11}\text{ZrO}_{40}$, are consistent with homolytic oxidation mechanisms (*vide supra*). No alteration of the reaction mechanism occurs while increasing amount of protons in Zr-POM. Importantly, **3** containing no acid protons reacts with neither H_2O nor H_2O_2 and shows low if any catalytic activity in the reactions with H_2O_2.

8. Summary and outlook

The results summarized in this paper demonstrate that TM-monosubstituted POMs show catalytic and spectroscopic performance similar to that observed for the corresponding heterogeneous TM-single-site catalysts and thus can serve as a useful tool to understand better processes occurring over solid catalysts. The following main conclusions can be drawn from the Ti-POM-based model studies: (1) Ti=O bond reacts with H_2O_2 slowly to give inactive peroxo complex "Ti(O)$_2$", while Ti–OH bond reacts fast to yield active protonated peroxo (hydroperoxo) complex "HTi(O)$_2$", therefore the formation of titanyl groups in titanium single-site catalysts should be avoided; (2) dimeric titanium species is able to catalyze H_2O_2-based oxidations but H_2O is needed to hydrolyze Ti–O–Ti bond to produce Ti–OH; (3) monoprotonated peroxotitanium complex **I** has a η^2-structure. In solid state, the activating proton is mostly localized at Ti–O–W bridging oxygen; however, both η^2- and η^1-species could coexist in solution; (4) **I** reacts with organic substrates via homolytic oxidation mechanisms; (5) the oxidation mechanism changes from homolytic to heterolytic when the amount of protons in
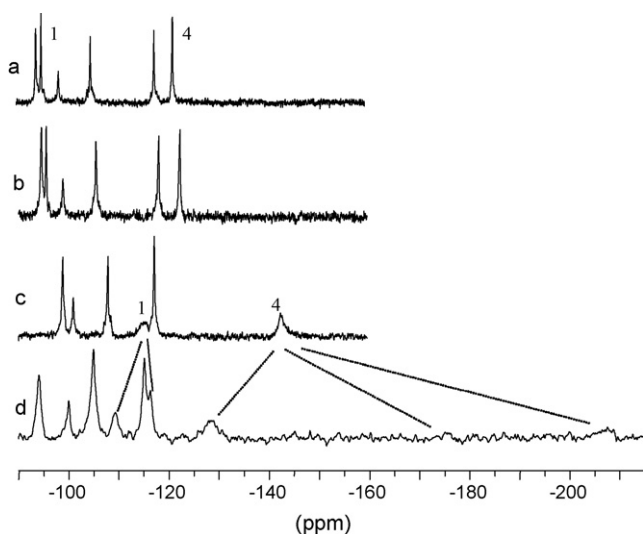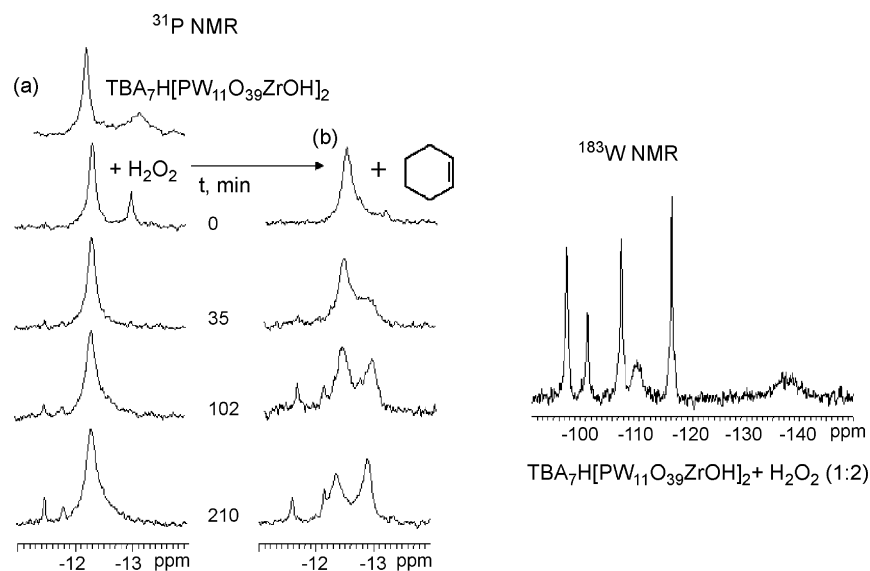
Fig. 14. Interaction of Zr-POM with H_2O_2 followed by ^{31}P (a: in the absence; b: in the presence of CyH) and ^{183}W NMR.

the Ti-POM peroxo complex (initial Ti-POM) increases from 1 to 2 per Ti atom; (6) Brőnsted acidity is crucial for the activity of Ti-single-site catalysts in oxidations with H_2O_2.

The model study based on Zr-POMs have demonstrated that the presence of acid protons is also vital for the activity of zirconium single-site catalysts, but in contrast to titanium, only homolytic oxidation mechanisms may operate with Zr. The formation of monomeric Zr(IV) species seems to be important for H_2O_2 activation. While Ti–O–Ti dimers easily react with water to produce highly reactive monomeric Ti–OH species, Zr–O–Zr bond is resistant to aqueous hydrolysis in the absence of acid protons. Therefore, both the formation of dimeric species and deprotonation should be avoided during preparation of Zr-single-site catalysts.

The approach that we suggest for studying oxidation mechanisms using TM-POMs as molecular models takes advantage of at least three facts. First, POM units can function as multidentate totally inorganic, thermodynamically stable ligands for redox-active TM ions. This provides advantages for POM-based model systems with respect to model systems based on TM-complexes with organic and organometallic ligands prone to oxidative degradation and/or hydrolysis. Second, the fundamental properties of POMs, including elemental composition, redox potentials, solubility, charge density, acidity, size, shape, etc., that impact their catalytic performance can be systematically altered. This makes them good objects for studying composition/structure/activity relationships. Third, POMs can be comprehensively investigated at the atomic level, both structurally and mechanistically. All these advantages would implement studying elementary steps of complicated oxidation processes and would help to answer the questions essential for successful designing an optimal catalytic centre for a given reaction: (1) which kinds of bonds (M=O, M–OH, M ← OH_2, M–O–M, M–O(H)–O, etc.) may exist for a specific M and how do they react with the specific oxidants (relative reactivity, mode of binding, etc.); (2) what active species are

formed upon interaction with the oxidant and how does their structure impact the reactivity and selectivity; (3) whether the substrate is activated by the metal centre or not, and what are the reactive intermediates; (4) what is the intimate mechanism of the interaction between the activated oxidant and a substrate within the reactive intermediate, and how can one affect the mechanism to govern the reaction selectivity, etc. In parallel with spectroscopic (especially, *in situ*) studies on heterogeneous TM-single-site catalysts, studying the structure and reactivity of well-defined TM-POMs using both experimental and computational methods would contribute toward understanding the elementary steps of heterogeneous reactions, particularly with respect to surface-bound intermediates.

Although many important aspects of Zr- and especially Ti-single-site catalysis have become clear in view of our POM-based model studies, it is apparent that a great number of opportunities, challenges, and applications are still to be expected. Among the questions that should be addressed in the nearest future are those about the size and geometry of an optimal titanium (other TM) cluster, about possibility of such clusters to activate both the oxidant and substrate molecules, about the structures of reactive intermediates, about the specific role of the activating protons, etc. In view of the growing number of new POMs, including various di-, tri- and other titanium-substituted polyoxotungstates [172,182,206, 212–221], new interesting model studies are becoming possible, and we anticipate these model studies will favor the progress in the field of molecular designing new efficient selective oxidation catalysts.

Acknowledgements

References

[1] R.A. Sheldon, J.K. Kochi, Metal-Catalyzed Oxidations of Organic Compounds, Academic Press, New York, 1981.

[2] G. Strukul (Ed.), Catalytic Oxidations with Hydrogen Peroxide as Oxidant, Kluwer Academic Publishers, Dordrecht, Boston, 1992.

[3] G.W. Parshall, S.D. Ittel, Homogeneous Catalysis: The Applications and Chemistry of Catalysis by Soluble Transition Metal Complexes, 2nd ed., Wiley–Interscience, New York, 1992.

[4] P.T. Anastas, J.C. Warner, Green Chemistry: Theory and Practice, Oxford University Press, New York, 1998.

[5] C.W. Jones, Application of Hydrogen Peroxide and Derivatives, Royal Society of Chemistry, London, 1999.

[6] A.E. Shilov, G.B. Shul'pin, in: B.R. James (Ed.), Activation Catalytic Reactions of Saturated Hydrocarbons in the Presence of Metal Complexes, Kluwer, Dordrecht, 2000.

[7] G. Centi, F. Cavani, F. Trifirro, Selective Oxidation by Heterogeneous Catalysis, Kluwer Academic/Plenum Publishers, New York, 2001.

[8] R.A. Sheldon, H. van Bekkum (Eds.), Fine Chemicals through Heterogeneous Catalysis, Wiley–VCH, Weinheim, 2001.

[9] P. Arpentinier, F. Cavani, F. Trifiro, The Technology of Catalytic Oxidations, Editions TECHNIP, Paris, 2001.

[10] I.T. Horvath (Ed.), Encyclopedia of Catalysis, vol. 6, Wiley–Interscience, New Jersey, 2003.

[11] R.A. Sheldon, J. Dakka, Catal. Today 19 (1994) 215.

[12] B. Notari, Adv. Catal. 41 (1996) 253 (and references therein).

[13] K. Sato, M. Aoki, R. Noyori, Science 281 (1998) 1646.

[14] M.G. Clerici, Top. Catal. 13 (2000) 373.

[15] W.R. Sanderson, Pure Appl. Chem. 72 (2000) 1289.

[16] J.S. Rafelt, J.H. Clark, Catal. Today 57 (2000) 33.

[17] B.M. Choudary, M.L. Kantam, P.L. Santhi, Catal. Today 57 (2000) 17.

[18] W.F. Hölderich, Catal. Today 62 (2000) 115.

[19] G.-J. Brink, I.W.C.E. Arends, R.A. Sheldon, Science 287 (2000) 1636.

[20] J.-M. Bregeault, Dalton Trans. (2003) 3289.

[21] G. Centi, S. Perathoner, Catal. Today 77 (2003) 287.

[22] G. Grigoropoulou, J.H. Clark, J.A. Elings, Green Chem. 5 (2003) 1.

[23] R. Noyori, M. Aoki, K. Sato, Chem. Commun. (2003) 1977.

[24] B.S. Lane, K. Burgess, Chem. Rev. 103 (2003) 2457.

[25] R. Neumann, in: M. Beller, C. Bolm (Eds.), Transition Metals for Organic Synthesis, vol. 2, 2nd ed., Wiley–VCH, Weinheim, 2004, p. 415.

[26] R. Neumann, in: J.-E. Baeckvall (Ed.), Modern Oxidation Methods, Wiley–VCH, Weinheim, 2004, p. 223.

[27] C.L. Hill, Angew. Chem. 43 (2004) 402 (and references therein).

[28] W. Adam (Ed.), Peroxide Chemistry, Wiley–VCH, Weinheim, 2000.

[29] M.G. Clerici, TS-1 and propylene oxide, 20 years later, in: Proceedings of the DGMK/SCI Conference "Oxidation and Functionalisation: Classical and Alternative Routes and Sources", October 12–14, Milan, Italy, 2005, pp. 165–176.

[30] Large Pore Molecular Sieves, special issue of Catal Today, 19 1994.

[31] G. Centi (Ed.), Catalysis by Unique Metal Ion Structures in Solid Matrices, Kluwer, The Netherlands, 2001.

[32] G. Bellussi, M.S. Rigutto, Stud. Surf. Sci. Catal. 85 (1994) 177.

[33] M. Hartmann, L. Kewvan, Chem. Rev. 99 (1999) 635.

[34] P.T. Tanev, M. Chibwe, T.J. Pinnnavaia, Nature 368 (1994) 321.

[35] T. Maschmeyer, F. Rey, G. Sankar, J.M. Thomas, Nature 378 (1995) 159.

[36] A. Sayari, Chem. Mater. 8 (1996) 1840.

[37] A. Corma, Chem. Rev. 97 (1997) 2373.

[38] X. Gao, I.E. Wachs, Catal. Today 51 (1999) 233.

[39] R.J. Saxton, Top. Catal. 9 (1999) 43.

[40] I.W.C.E. Arends, R.A. Sheldon, Appl. Catal. A: Gen. 212 (2001) 175.

[41] P. Selvam, S.K. Bhatia, C.G. Sonwane, Ind. Eng. Chem. Res. 40 (2001) 3237.

[42] D.E. De Vos, M. Dams, B.F. Sels, P.A. Jacobs, Chem. Rev. 102 (2002) 3615.

[43] M. Ziolek, Catal. Today 90 (2004) 145.

[44] B. Viswanathan, B. Jacob, Catal. Rev. Sci. Eng. 47 (2005) 1.

[45] A. Taguchi, F. Schuth, Micropor. Mesopor. Mater. 77 (2005) 1.

[46] P. Ratnasamy, D. Srinivas, H. Knozinger, Adv. Catal. 48 (2004) 1–169.

[47] O.A. Kholdeeva, N.N. Trukhan, Russ. Chem. Rev. 75 (2006) 460.

[48] M. Taramasso, G. Perego, B. Notari, US Patent 4,410,501 (1983).

[49] C. Neri, B. Anfossi, A. Esposito, F. Buonomo, EP 100119, 1986.

[50] B. Notari, Stud. Surf. Sci. Catal. 37 (1988) 413.

[51] M.G. Clerici, Appl. Catal. 68 (1991) 249.

[52] G. Bellussi, A. Cazati, M.G. Clerici, G. Maddinelli, R. Millini, J. Catal. 133 (1992) 220.

[53] M.G. Clerici, P. Ingallina, J. Catal. 140 (1993) 71.

[54] M.K. Dongare, P. Singh, P.P. Moghe, P. Ratnasamy, Zeolites 11 (1991) 690.

[55] M. Besson, M.C. Bonnet, P. Gallezot, I. Tkachenko, A. Tuel, Catal. Today 51 (1999) 547.

[56] K. Chaudhari, R. Bal, D. Srinivas, A.J. Chandwadkar, S. Sivasanker, Micropor. Mesopor. Mater. 50 (2001) 209.

[57] X.-X. Wang, L. Veyre, F. Lefebvre, J. Patarin, J.-M. Basset, Micropor. Mesopor. Mater. 66 (2003) 169.

[58] C. Palazzi, L. Oliva, M. Signoretto, G. Strukul, J. Catal. 194 (2000) 286.

[59] M.J. Morandin, R. Gavagnin, F. Pinna, G. Strukul, J. Catal. 212 (2002) 193.

[60] N.V. Maksimchuk, M.S. Melgunov, J. Mrowiec-Białoń, A.B. Jarzębski, O.A. Kholdeeva, J. Catal. 235 (2005) 175.

[61] J.M. Thomas, J. Mol. Catal. A: Chem. 115 (1997) 371.

[62] J.M. Thomas, C.R.A. Catlow, G. Sankar, Chem. Commun. (2002) 2921.

[63] F. Lefebvre, J.-M. Basset, Curr. Top. Catal. 3 (2002) 215.

[64] T. Don Tilley, J. Mol. Catal. A: Chem. 182/183 (2002) 17.

[65] M.A. Barteau, J.E. Lyons, J. Catal. 216 (2003) 236.

[66] J.M. Thomas, R. Raja, J. Organomet. Chem. 689 (2004) 4110.

[67] J.-M. Basset, J.-P. Candy, C. Coperet, F. Lefebvre, E.A. Quadrelli, Nanotechnol. Catal. 2 (2004) 447.

[68] A. Zecchina, S. Bordiga, C. Lamberti, G. Ricchiardi, D. Scarano, G. Petrini, G. Leofanti, M.A. Mantegazza, Catal. Today 32 (1996) 97.

[69] V. Bolis, S. Bordiga, C. Lamberti, A. Zecchina, A. Carati, F. Rivetti, G. Spano, G. Petrini, Langmuir 15 (1999) 5753.

[70] G. Tozzola, M.A. Mantegazza, G. Ranghino, G. Petrini, S. Bordiga, G. Ricchiardi, C. Lamberti, R. Zulian, A. Zecchina, J. Catal. 179 (1998) 64.

[71] I.V. Yudanov, P. Gisdakis, C. Di Valentin, N. Rosch, Eur. J. Inorg. Chem. 12 (1999) 2135.

[72] G.M. Zhidomirov, A.L. Yakovlev, M.A. Milov, N.A. Kachurovskaya, I.V. Yudanov, Catal. Today 51 (1999) 397.

[73] J.M. Thomas, G. Sankar, Acc. Chem. Res. 34 (2001) 571.

[74] H. Munakata, Y. Oumi, A. Miyamoto, J. Phys. Chem. B 105 (2001) 3493.

[75] A. Zecchina, S. Bordiga, G. Spoto, A. Damin, G. Berlier, F. Bonino, C. Prestipino, C. Lamberti, Top. Catal. 21 (2002) 67 (and references therein).

[76] S. Bordiga, A. Damin, F. Bonino, G. Ricchiardi, C. Lambertim, A. Zecchina, Angew. Chem. Int. Ed. 41 (2002) 4734.

[77] C.M. Barker, D. Gleeson, N. Kaltsoyannis, C.R.A. Catlow, G. Sankar, J.M. Thomas, Phys. Chem. Chem. Phys. 4 (2002) 1228.

[78] G. Sankar, J.M. Thomas, C.R.A. Catlow, C.M. Barker, D. Gleeson, N. Kaltsoyannis, J. Phys. Chem. B 107 (2003) 1932.

[79] S.O. Lee, R. Raja, K.D.M. Harris, J.M. Thomas, B.F.G. Johnson, G. Sankar, Angew. Chem. Int. Ed. 42 (2003) 1520.

[80] R.R. Sever, T.W. Root, J. Phys. Chem. 107 (2003) 4080.

[81] C. Prestipino, F. Bonino, S. Usseglio, A. Damin, A. Tasso, M.G. Clerici, S. Bordiga, F. D'Acapito, A. Zecchina, C. Lamberti, Chem. Phys. Chem. 5 (2004) 1799.

[82] F. Bonino, A. Damin, G. Ricchiardi, M. Ricci, G. Spano, R. D'Aloisio, A. Zecchina, C. Lamberti, C. Prestipino, S. Bordiga, J. Phys. Chem. B 108 (2004) 3573.

[83] F. Feher, J. Am. Chem. Soc. 108 (1986) 3850.

[84] H. Arzoumanian, A. Baldi, R. Lay, M. Pierrot, J.F. Petrignani, F. Ridouane, J. Sanchez, H. Krentzien, in: W. Ando, Y. Moro-oka (Eds.), The Role of Oxygen in Chemistry and Biochemistry, Studies in Organic Chemistry, vol. 33, Elsevier, Amsterdam, 1988, p. 227.

[85] J.-M. Basset, J.-P. Candy, A. Choplin, B. Didillon, F. Quignard, A. Theolier, in: J.M. Thomas, K.I. Zamaraev (Eds.), Perspectives in Catalysis, Blackwell, Oxford, 1991, p. 125.

[86] F.T. Edelmann, Angew. Chem. Int. Ed. 31 (1992) 586.

[87] J.-M. Basset, F. Lefebvre, C. Cantini, Coord. Chem. Rev. 178–180 (1998) 1703.

[88] V. Lorenz, A. Fischer, S. Gießmann, J.W. Gilje, Y. Gun'ko, K. Jacob, F.T. Edelmann, Coord. Chem. Rev. 206-207 (2000) 321.

[89] H.W. Roesky, I. Haiduc, N.S. Hosmane, Chem. Rev. 103 (2003) 2579.

[90] R. Fandos, A. Otero, A. Rodriguez, M.J. Ruiz, P. Trreros, Angew. Chem. Int. Ed. 40 (2001) 2884.

[91] R. Duchateau, Chem. Rev. 102 (2002) 3525.

[92] E.P. Talsi, D.E. Babushk, J. Mol. Catal. A: Chem. 106 (1996) 179.

[93] M. Crocker, R.H.M. Herold, A.G. Orpen, Chem. Commun. (1997) 2411.

[94] M. Crocker, R.H.M. Herold, A.G. Orpen, T.A. Overgaag, J. Chem. Soc., Dalton Trans. (1999) 3791.

[95] J.M. Thomas, G. Sankar, M.C. Klunduk, M.P. Attfield, T. Maschmeyer, B.F.G. Johnson, R.G. Bell, J. Phys. Chem. B 103 (1999) 8809.

[96] M. Chabanas, E.A. Quadrelli, B. Fenet, C. Coperet, J. Thivolle-Cazat, J.-M. Basset, A. Lesage, L. Emsley, Angew. Chem. Int. Ed. 40 (2001) 4493.

[97] P.P. Pescarmona, J.C. Van der Waal, I.E. Maxwell, T. Maschmeyer, Angew. Chem. Int. Ed. 40 (2001) 740.

[98] M. Fujiwara, H. Wessel, P. Hyung-Suh, H.W. Roesky, Tetrahedron 58 (2002) 239.

[99] M.T. Pope, Heteropoly and Isopoly Oxometalates, Springer-Verlag, New York, 1983.

[100] M.T. Pope, A. Müller (Eds.), Polyoxometalates: From Platonic Solids to Anti-Retroviral Activity, Kluwer, Dordrecht, The Netherlands, 1993.

[101] M.T. Pope, A. Müller (Eds.), Polyoxometalate Chemistry: From Topology via Self-Assembly to Applications, Kluwer, Dordrecht, The Netherlands, 2001.

[102] J.B. Moffat, Metal–Oxygen Clusters: The Surface and Catalytic Properties of Heteropoly Oxometalates, Kluwer/Plenum, New York, 2001.

[103] J.J. Borrás-Almenar, E. Coronado, A. Müller, M.T. Pope (Eds.), Polyoxometalate Molecular Science, Kluwer, Dordrecht, The Netherlands, 2003.

[104] J. Mol. Catal. 114 (1–3) (1996), special issue on POMs.

[105] Chem. Rev. 98 (1998), special issue on POMs.

[106] C.L. Hill, C.M. Prosser-McCartha, Coord. Chem. Rev. 143 (1995) 407.

[107] R. Neumann, Prog. Inorg. Chem. 47 (1998) 317.

[108] M.T. Pope, Polyoxo anions: synthesis and structure, in: A.G. Wedd (Ed.), Comprehensive Coordination Chemistry II, vol. 4, Elsevier Science, New York, 2004, p. 635.

[109] C.L. Hill, Polyoxometalates: reactivity, in: A.G. Wedd (Ed.), Comprehensive Coordination Chemistry II, vol. 4, Elsevier Science, New York, 2004, p. 679.

[110] C.L. Hill, R.B. Brown, J. Am. Chem. Soc. 108 (1986) 536.

[111] D.E. Katsoulis, M.T. Pope, J. Chem. Soc. Chem. Commun. (1986) 1186.

[112] L.C.W. Baker, in: S. Kirschner (Ed.), Advances in the Chemistry of Coordination Compounds, Macmillan, New York, 1961.

[113] V.W. Day, W.G. Klemperer, Science 228 (1985) 533.

[114] R.G. Finke, M.W. Droege, J. Am. Chem. Soc. 106 (1984) 7274.

[115] R.G. Finke, B. Rapko, Organometallics 4 (1985) 175.

[116] R.G. Finke, B. Rapko, R.J. Saxton, P.J. Domaille, J. Am. Chem. Soc. 108 (1986) 2947.

[117] M. Fournier, C. Louis, M. Che, P. Chaquin, D. Masure, J. Catal. 119 (1989) 400.

[118] M.T. Pope, A. Müller, Angew. Chem. Int. Ed. 30 (1991) 34.

[119] Q. Chen, J. Zubieta, Coord. Chem. Rev. 114 (1992) 107.

[120] L.C.W. Baker, D.C. Glick, Chem. Rev. 98 (1998) 3.

[121] T.R. Mohs, Y. Du, B. Plashko, E.A. Maatta, Chem. Commun. (1997) 1707.

[122] L. Ma, S. Liu, J. Zubieta, Inorg. Chem. 28 (1989) 175.

[123] R. Villanneau, H. Carabineiro, X. Carrier, R. Thouvenot, P. Herson, F. Lemos, F.R. Ribeiro, M. Che, J. Phys. Chem. B 108 (2004) 12465.

[124] O.A. Kholdeeva, R.I. Maksimovskaya, G.M. Maksimov, K.I. Zamaraev, React. Kinet. Catal. Lett. 63 (1998) 95.

[125] O.A. Kholdeeva, G.M. Maksimov, R.I. Maksimovskaya, L.A. Kovaleva, M.A. Fedotov, React. Kinet. Catal. Lett. 66 (1999) 311.

[126] O.A. Kholdeeva, L.A. Kovaleva, R.I. Maksimovskaya, G.M. Maksimov, J. Mol. Catal. A: Chem. 158 (2000) 223.

[127] O.A. Kholdeeva, G.M. Maksimov, R.I. Maksimovskaya, L.A. Kovaleva, M.A. Fedotov, V.A. Grigoriev, C.L. Hill, Inorg. Chem. 39 (2000) 3828.

[128] O.A. Kholdeeva, R.I. Maksimovskaya, G.M. Maksimov, L.A. Kovaleva, Kinet. Katal. 42 (2001) 1.

[129] O.A. Kholdeeva, T.A. Trubitsina, R.I. Maksimovskaya, A.V. Golovin, W.A. Neiwert, B.A. Kolesov, X. López, J.-M. Poblet, Inorg. Chem. 43 (2004) 2284.

[130] O.A. Kholdeeva, T.A. Trubitsina, G.M. Maksimov, A.V. Golovin, R.I. Maksimovskaya, Inorg. Chem. 44 (2005) 1635.

[131] O.A. Kholdeeva, T.A. Trubitsina, M.N. Timofeeva, G.M. Maksimov, R.I. Maksimovskaya, V.A. Rogov, J. Mol. Catal. A: Chem. 232 (2005) 173.

[132] O.A. Kholdeeva, G.M. Maksimov, R.I. Maksimovskaya, M.P. Vanina, T.A. Trubitsina, D.Yu. Naumov, B.A. Kolesov, N.S. Antonova, J.J. Carbo, J.M. Poblet, Inorg. Chem. 45 (2006) 7224.

[133] T. Blasco, A. Corma, M.T. Navarro, J.P. Pariente, J. Catal. 156 (1995) 65.

[134] D.C. Dutoit, M. Schneider, R. Hutter, A. Baiker, J. Catal. 161 (1996) 651.

[135] L.Y. Chen, G.K. Chuah, S. Jaenicke, Catal. Lett. 50 (1998) 107.

[136] J.M. Fraile, J.I. Garcia, J.A. Mayoral, E. Vispe, J. Catal. 189 (2000) 40.

[137] P. Wu, T. Tatsumi, T. Komatsu, T. Yashima, J. Catal. 202 (2001) 245.

[138] W.-S. Ahn, N.-K. Kim, S.-Y. Jeong, Catal. Today 68 (2001) 83.

[139] O.A. Kholdeeva, A.Yu. Derevyankin, A.N. Shmakov, N.N. Trukhan, E.A. Paukshtis, A. Tuel, V.N. Romannikov, J. Mol. Catal. A: Chem. 158 (2000) 417.

[140] N.N. Trukhan, A.Yu. Derevyankin, A.N. Shmakov, E.A. Paukshtis, O.A. Kholdeeva, V.N. Romannikov, Micropor. Mesopor. Mater. 44/45 (2001) 603.

[141] S.C. Laha, R. Kumar, Micropor. Mesopor. Mater. 53 (2002) 163.

[142] M. Swegler, M. Floor, H. Van Bekkum, Tetrahedron Lett. 29 (1988) 823.

[143] N.I. Kuznetsova, L.G. Detusheva, L.I. Kuznetsova, M.A. Fedotov, V.A. Likholobov, Kinet. Katal. 33 (1992) 516.

[144] T. Yamase, E. Ishikawa, Y. Asai, S. Kanai, J. Mol. Catal. A: Chem. 114 (1996) 237.

[145] A.C. Dengel, W.P. Griffith, B.C. Parkin, J. Chem. Soc., Dalton Trans. (1993) 2683.

[146] L. Salles, C. Aubry, R. Thouvenot, F. Robert, C. Doremieux-Morin, G. Chottard, H. Ledon, Y. Jeannin, J.-M. Brégeault, Inorg. Chem. 33 (1994) 871.

[147] D.C. Duncan, R.C. Chambers, E. Hecht, C.L. Hill, J. Am. Chem. Soc. 117 (1995) 681.

[148] C. Venturello, R. D'Aloisio, J.C.R. Bart, M. Ricci, J. Mol. Catal. 32 (1985) 107.

[149] C. Venturello, R. D'Aloisio, J. Org. Chem. 53 (1988) 1553.

[150] N.N. Trukhan, V.N. Romannikov, E.A. Paukshtis, A.N. Shmakov, O.A. Kholdeeva, J. Catal. 202 (2001) 110.

[151] O.A. Kholdeeva, N.N. Trukhan, M.P. Vanina, V.N. Romannikov, V.N. Parmon, J. Mrowiec-Białoń, A.B. Jarzębski, Catal. Today 75 (2002) 203.

[152] J. Mrowiec-Białoń, A.B. Jarzębski, O.A. Kholdeeva, N.N. Trukhan, V.I. Zaikovski, V.V. Kriventsov, Z. Olejniczak, Appl. Catal. A: Gen. 273 (2004) 47.

[153] O.A. Kholdeeva, M.S. Melgunov, A.N. Shmakov, N.N. Trukhan, V.V. Kriventsov, V.I. Zaikovskii, V.N. Romannikov, Catal. Today 91/92 (2004) 205.

[154] O.A. Kholdeeva, M.P. Vanina, J. Mrowiec-Białoń, A.B. Jarzębski, unpublished results.

[155] N.N. Trukhan, O.A. Kholdeeva, Kinet. Katal. 44 (2003) 1.

[156] T.A. Trubitsina, O.A. Kholdeeva, Kinet. Katal., submitted for publication.

[157] R.S. Reddy, J.S. Reddy, R. Kumar, P. Kumar, J. Chem. Soc., Chem. Commun. (1992) 84.

[158] A. Corma, M. Iglesias, F. Sanchez, Catal. Lett. 39 (1996) 153.

[159] R.D. Gall, M. Faraj, C.L. Hill, Inorg. Chem. 33 (1994) 5015.

[160] O. Bortolini, F. Di Furia, G. Modena, J. Mol. Catal. 16 (1982) 61.

[161] A.G.J. Ligtenbarg, R. Hage, B.L. Feringa, Coord. Chem. Rev. 237 (2003) 89.

[162] E. Baciocchi, O. Lanzalunga, S. Malandrucco, J. Am. Chem. Soc. 118 (1996) 8973.

[163] E. Baciocchi, E. Fessela, O. Lanzalunga, M. Mattioli, Angew. Chem. Int. Ed. Engl. 32 (1993) 1071.

[164] C. Tourné, Compt. Rend. Acad. Sci., Ser. C 226 (1968) 702.

[165] R.K.C. Ho, W.G. Klemperer, J. Am. Chem. Soc. 100 (1978) 6772.

[166] W.H. Knoth, J. Am. Chem. Soc. 101 (1979) 759.

[167] W.H. Knoth, P.J. Domaille, D.C. Roe, Inorg. Chem. 22 (1983) 198.

[168] G.M. Maksimov, L.I. Kuznetsova, K.I. Matveev, R.I. Maksimovskaya, Koord. Khim. 11 (1985) 1353 (in Russian).

[169] T. Yamase, T. Ozeki, S. Motomura, Bull. Chem. Soc. Jpn. 65 (1992) 1453.

[170] J.F.W. Keana, M.D. Ogan, J. Am. Chem. Soc. 108 (1986) 7951.

[171] L.-Y. Qu, Q.-J. Shan, J. Gong, R.-Q. Lu, D.-R. Wang, J. Chem. Soc., Dalton Trans. (1997) 4525.

[172] U. Kortz, S.S. Hamzeh, N.A. Nasser, Chem. Eur. J. 9 (2003) 2945.

[173] W. Clegg, M.R.J. Elsegood, R.J. Errington, J. Havelock, J. Chem. Soc., Dalton Trans. (1996) 681.

[174] L. Meng, X. Zhan, Transit. Metal Chem. 26 (2001) 448.

[175] Y.G. Chen, J.F. Liu, Polyhedron 15 (1996) 3433.

[176] Y.G. Chen, J.F. Liu, Synth. React. Inorg. Met. Org. Chem. 27 (1997) 239.

[177] J.A. Fernandez, X. Lopez, J.M. Poblet, J. Mol. Catal. A: Chem. 262 (2007) 236–242.

[178] G.M. Maksimov, R.I. Maksimovskaya, I.V. Kozhevnikov, Zh. Neorgan. Khim. 37 (1992) 2279.

[179] M. Inamoto, S. Funahashi, M. Tanaka, Inorg. Chim. Acta 76 (1983) L93.

[180] M. Crocker, K.A. Emeis, R.H.M. Herold, J. Mol. Catal. 110 (1996) L7.

[181] H.J. Ledon, F. Varescon, Inorg. Chem. 23 (1984) 2735.

[182] Y. Sakai, Y. Kitakoga, K. Hayashi, K. Yoza, K. Nomiya, Eur. J. Inorg. Chem. (2004) 4646.

[183] H. Mimoun, M. Postel, F. Casabianca, J. Fisher, A. Mitschler, Inorg. Chem. 21 (1982) 1303.

[184] V.L. Goedken, J.A. Ladd, J. Chem. Soc., Chem. Commun. (1982) 142.

[185] M. Postel, F. Casabianca, Y. Gauffreteau, Inorg. Chim. Acta 113 (1986) 173.

[186] M.F. Sisemore, M. Selke, J.N. Burstyn, J.S. Valentine, Inorg. Chem. 36 (1997) 979.

[187] G. Schwarzenbach, Inorg. Chem. 9 (1970) 2391.

[188] J. Muhlebach, K. Muller, G. Schwarzenbach, Inorg. Chem. 9 (1970) 2381.

[189] A. Butler, M.J. Clague, G.E. Meister, Chem. Rev. 94 (1994) 625.

[190] J.-M. Latour, B. Galland, J.-C. Marchon, J. Chem. Soc., Chem. Commun. (1979) 570.

[191] M.S. Reynolds, A. Butler, Inorg. Chem. 35 (1996) 2378.

[192] W.P. Griffith, T.D. Wickins, J. Chem. Soc. (A) (1968) 397.

[193] E.M. Nour, S. Morsy, Inorg. Chim. Acta 117 (1986) 45.

[194] M. Kakihana, M. Tada, M. Shiro, V. Petrykin, M. Osada, Y. Nakamura, Inorg. Chem. 40 (2001) 891.

[195] M. Dakanali, E.T. Kefalas, C.P. Raptopoulou, A. Terzis, G. Voyiatzis, I. Kyrikou, T. Mavromoustakos, A. Salifoglou, Inorg. Chem. 42 (2003) 4632.

[196] J.G. Highfield, J.B. Moffat, J. Catal. 88 (1984) 177.

[197] G.A. Jeffrey, An Introduction to Hydrogen Bonding, Oxford University Press, New York, 1997, p. 303.

[198] D.L. Kepert, The Early Transition Metals, Academic Press, London, 1972, p. 47.

[199] M.-M. Rohmer, M. Bénard, J.-P. Blaudeau, J.M. Maestre, J.M. Poblet, Coord. Chem. Rev. 178–180 (1998) 1019.

[200] J.M. Maestre, J.P. Sarasa, C. Bo, J.M. Poblet, Inorg. Chem. 37 (1998) 3071.

[201] X. López, C. Bo, J.M. Poblet, J. Am. Chem. Soc. 124 (2002) 12574.

[202] C.C. Pye, T. Ziegler, Theor. Chem. Acc. 101 (1999) 396.

[203] R.Y.N. Ho, G. Roelfes, B.L. Feringa, L. Que, J. Am. Chem. Soc. 121 (1999) 264.

[204] A.J. Simaan, S. Dopner, F. Banse, S. Bourcier, G. Bouchoux, A. Boussac, P. Hilderbrandt, J.-J. Girerd, Eur. J. Inorg. Chem. (2000) 1627.

[205] RU Patent 2196764, 2001;
RU Patent 2229930, 2004.

[206] C.N. Kato, S. Negishi, K. Yoshida, K. Hayashi, K. Nomiya, Appl. Catal. A: Gen. 292 (2005) 97.

[207] F. Chiker, J.-F. Nogier, F. Launay, J.-L. Bonardet, Appl. Catal. A: Gen. 243 (2003) 309.

[208] F. Chauveau, J. Eberle, J. Lefebvre, Nouv. J. Chim. 9 (1985) 315.

[209] R.J. Errington, in: J.J. Borrás-Almenar, E. Coronado, A. Müller, M.T. Pope (Eds.), Polyoxometalate Molecular Science, Kluwer, Dordrecht, The Netherlands, 2003, p. 55.

[210] A.J. Gaunt, I. May, D. Collison, K.T. Holman, M.T. Pope, J. Mol. Struct. 656 (2003) 101.

[211] X. Fang, T. Anderson, C.L. Hill, Angew. Chem. Int. Ed. 44 (2005) 3540.

[212] Y. Lin, T.J.R. Weakley, R. Rapko, R.G. Finke, Inorg. Chem. 32 (1993) 5095.

[213] T. Yamase, T. Ozeki, H. Sakamoto, S. Nishiya, A. Yamamoto, Bull. Chem. Soc. Jpn. 66 (1993) 103.

[214] N.J. Crano, R.C. Chambers, V.M. Lynch, M.A. Fox, J. Mol. Catal. A: Chem. 114 (1996) 65.

[215] X.-H. Wang, J.-F. Liu, Y.-G. Chen, Q. Liu, J.-T. Liu, M.T. Pope, J. Chem. Soc., Dalton Trans. (2000) 1139.

[216] K. Nomiya, M. Takahashi, K. Ohsawa, J.A. Widegren, J. Chem. Soc., Dalton Trans. (2001) 2872.

[217] K. Nomiya, M. Takahashi, J.A. Widegren, T. Aizawa, Y. Sakai, N.C. Kasuga, J. Chem. Soc., Dalton Trans. (2002) 3679.

[218] Y. Sakai, K. Yoza, C.N. Kato, K. Nomiya, Dalton Trans. (2003) 3581.

[219] Y. Sakai, K. Yoza, C.N. Kato, K. Nomiya, Chem. Eur. J. 9 (2003) 4077.

[220] F. Hussain, B.S. Bassil, L.-H. Bi, M. Reicker, U. Kortz, Angew. Chem. Int. Ed. 43 (2004) 3485.

[221] K. Hayashi, M. Takahashi, K. Nomiya, Dalton Trans. (2005) 3751.